



**IMPROVING LOW ORDER, LINEAR, POSITIVE SPATIAL  
QUADRATURES FOR THE PARTIAL CURRENT NEUTRON TRANSPORT  
METHOD**

**THESIS**

John M Snyder, Major, USA

AFIT/GNE/ENP/10M-08

**DEPARTMENT OF THE AIR FORCE  
AIR UNIVERSITY**

**Air Force Institute of Technology**

---

---

**Wright-Patterson Air Force Base, Ohio**

APPROVED FOR PUBLIC RELEASE; DISTRIBUTION UNLIMITED

The views expressed in this thesis are those of the author and do not reflect the official policy or position of the United States Air Force, Department of Defense, or the U.S. Government.

AFIT/GNE/ENP/10M-M08

IMPROVING LOW ORDER, LINEAR, POSITIVE SPATIAL QUADRATURES  
FOR THE PARTIAL CURRENT NEUTRON TRANSPORT METHOD  
THESIS

Presented to the Faculty  
Department of Engineering Physics  
Graduate School of Engineering and Management  
Air Force Institute of Technology  
Air University  
Air Education and Training Command  
In Partial Fulfillment of the Requirements for the  
Degree of Master of Science

John M Snyder, B.S.  
Major, USA

March 2010

APPROVED FOR PUBLIC RELEASE; DISTRIBUTION UNLIMITED.

IMPROVING LOW ORDER, LINEAR, POSITIVE SPATIAL QUADRATURES  
FOR THE PARTIAL CURRENT NEUTRON TRANSPORT METHOD

John M Snyder, B.S.

Major, USA

Approved:



Kirk A. Mathews, PhD (Research Advisor)

Professor of Nuclear Engineering

10 March 2010

Date




for LtCol Kyle A. Novak, PhD (Member)

Asst. Professor of Mathematics

10 March 2010

Date



Cpt Benjamin R. Kowash, PhD (Member)

Asst. Professor of Nuclear Engineering

10 March 2010

Date

## Abstract

AFIT researchers have developed a new approach to solving Discrete Ordinates equations, which approximate the linear Boltzmann Transport Equation (BTE). The usual approach is von Neumann iteration on the scattering source, which requires repeated sweeps through the spatial-angular grid. Acceptable convergence requires complicated and expensive acceleration schemes. The new approach, Partial-Current Transport (PCT) with Adaptive Distribution Iteration, eliminates scattering source iteration through matrix inversions and a reduced-size global linear algebra problem. It creates the needed matrices directly from the standard spatial quadratures used in the sweeping.

Positivity, linearity, and (higher-than-first-order) accuracy are the key desirable qualities with all Discrete Ordinates methods, but all three, according to Lathrop [8], cannot be achieved simultaneously. If a high order accurate, linear method is used, it can produce negative fluxes. Non-linear methods have been developed that are high-order accurate and positive, but these methods are not widely accepted because the BTE is itself a linear equation. Positive, linear methods are available, but are only first-order accurate. The latter can achieve needed accuracy by using optically-thin cells, but with Source Iteration (SI), this requires a fine grid of many cells, hence large computational expense.

My new approach is to partition an optically thick cell into  $2^N$  identical sub-cells. Each sub-cell is optically thin enough that first-order accurate spatial quadrature methods are sufficiently accurate as well as being linear and positive. The needed matrices are computed as before for a (thinnest) sub-cell. My algorithm combines the matrices for a pair of sub-cells to get the matrices for a single (merged) sub-cell twice as thick. Merging  $N$  times yields the matrices for the original cell. This allows PCT to solve the discrete ordinates equations with linearity, positivity, and sufficient accuracy without the high computational cost of increasing the number of cells by a factor of  $2^N$ .

## **Acknowledgements**

I would like to express my sincere gratitude to my research advisor, Dr. Kirk Mathews, for his patience and for the innumerable hours he spent helping me understand transport theory. I am extremely grateful to my wife and children for their support over the last 18 months. Thanks also to my classmates for being there to help carry the load.

Mike Snyder

## Table of Contents

	Page
Abstract.....	vii
Acknowledgements .....	ix
Table of Contents.....	x
List of Figures .....	xii
List of Tables.....	xiii
List of Symbols.....	xiv
List of Abbreviations .....	xvi
I. INTRODUCTION .....	1
I.A. Background .....	3
I.A.1 Linearity .....	5
I.A.2 Positivity.....	5
I.A.3 Accuracy .....	6
I.A.4 Distribution Iteration.....	6
I.B. Motivation.....	7
I.C. Objectives.....	7
I.D. Statement of the Problem .....	8
I.E. Scope and Limitations .....	8
I.F. Approach .....	8
II. Theory.....	10
II.A. Angular Quadratures .....	11
II.B. Spatial Quadratures .....	12
II.C. Within-Cell Transport.....	13

	Page
II.C.1 Calculating the Within-Cell Transport Matrices .....	13
II.C.2 Merging Cells .....	19
III. Testing .....	27
III.A. Verification Testing .....	27
III.B. Performance Testing .....	29
III.B.1 Test Problem 1: Scattering Ratio ( $c$ ) = .25 .....	30
III.B.2 Test Problem 2: Scattering Ratio ( $c$ ) = .75 .....	31
III.B.3 Test Problem 3: No Source, Current in on One Side .....	33
III.B.4 Test Problem 4: Approaching Diffusion .....	35
III.C. Matrix Conditioning .....	37
III.C.1 Condition Number vs. Cell Thickness (Optical) ( $c = .1$ ) .....	37
III.C.2 Condition Number vs. Cell Thickness (Optical) ( $c = .9$ ) .....	38
III.C.3 Condition Number vs. Cell Thickness (Optical) ( $c = 1$ ) .....	40
III.C.4 Condition Number Dependence on Angular Quadrature .....	41
IV. Summary .....	42
IV.A. Achievement of Objectives .....	42
IV.B. Future Work .....	43
IV.C. Observations and Conclusions .....	43
Appendix A .....	44
K matrices for Step .....	44
Appendix B K matrices for step characteristic .....	45



## List of Figures

Figure	Page
Figure 1: Discrete Ordinates (S4) Representation .....	2
Figure 2: Within-Cell Transport .....	11
Figure 3: One Cell Currents .....	13
Figure 4: Original Cell .....	20
Figure 5: Cell Divided into Smallest Sub-cells .....	20
Figure 6: Merge #1 .....	20
Figure 7: Merge 1 Result .....	20
Figure 8: Merge #2 .....	21
Figure 9: Merge 2 Result .....	21
Figure 10: Merge #3 .....	21
Figure 11: Merge 3 Result .....	21
Figure 12: Currents in Split Cells .....	22
Figure 13: Test Problem 1: $c = .25$ .....	31
Figure 14: Test Problem 2: $c = .75$ .....	33
Figure 15: Test Problem 3: No Source, One Current .....	35
Figure 16: Test Problem 4: Approaching Diffusion .....	36

## List of Tables

Table	Page
Table 1: Spatial Quadrature Comparison .....	12
Table 2: SI vs. DI.....	<b>Error! Bookmark not defined.</b>
Table 3: Test Problem 1 Results.....	30
Table 4: Test Problem 2 Results.....	32
Table 5: Test Problem 4 Results.....	34
Table 6: Condition Number vs. Cell Thickness ( $c = 0.9$ ).....	39
Table 7: Condition Number vs. Cell Thickness ( $c = 1$ ) .....	40

## List of Symbols

Symbol	Page
$\mu_n$	Direction Cosine for Ordinate n..... 2
$S_n$	Discrete Ordinates Angular Approximation..... 2
$v$	Neutron Velocity..... 8
$t$	Time..... 8
$\hat{\Omega}$	Direction..... 8
$E$	Energy..... 8
$\nabla$	Divergence Operator..... 8
$\sigma$	Total Cross Section..... 8
$\vec{r}$	Position Vector..... 8
$q$	Rate Density..... 8
$\psi$	Angular Flux..... 8
$\phi$	Scalar Flux..... 8
$\sigma_s$	Differential Scattering Cross Section..... 8
$\vec{j}^{out}$	Cell Outflow Currents..... 8
$\vec{j}^{in}$	Cell Inflow Current..... 8
$\psi_A$	Average Cell Angular Flux..... 8
$\vec{S}^{ext}$	External Emission Source..... 8
$\mathbf{K}^{\psi,I}$	Cell Inflow to Cell Flux Matrix..... 12
$\mathbf{K}^{\psi,E}$	Cell Emission to Cell Flux Matrix..... 12
$\mathbf{K}^{\psi,S}$	Cell Scatter to Cell Flux Matrix..... 12
$\vec{S}^S$	Cell Source Due to Scatter Matrix..... 12
$\Sigma^{S,\psi}$	Cell Scattering Matrix..... 12
$\mathbf{I}$	Identity Matrix..... 12
$\mathbf{L}$	Within Cell Scattering Matrix..... 12
$\mathbf{m}^{\psi,in}$	Cell Inflow to Cell Flux Transport Matrix..... 13

Symbol	Page
$\mathbf{m}^{\psi,ext}$ Cell Source to Cell Flux Transport Matrix.....	13
$\mathbf{K}^{O,I}$ Cell Inflow to Cell Outflow Matrix.....	13
$\mathbf{K}^{O,E}$ Cell Emission to Cell Outflow Matrix.....	13
$\mathbf{K}^{O,S}$ Cell Scatter to Cell Outflow Matrix.....	13
$\mathbf{m}^{out,in}$ Cell Inflow to Cell Outflow Transport Matrix.....	13
$\mathbf{m}^{out,ext}$ Cell Emission to Cell Outflow Transport Matrix.....	13
$\mathbf{T}_{\psi}^{-+}$ Negative to Negative Transmission from Flux Sub-Matrix.....	17
$\mathbf{T}_j^{--}$ Negative to Negative Transimmion from Current Sub-Matrix.....	17
$\mathbf{R}_j^{-+}$ Positive to Negative Reflection from Current Sub-Matrix.....	17
$\mathbf{R}_j^{+-}$ Negative to Positive Reflection from Current Sub-Matrix.....	17
$\mathbf{T}_j^{++}$ Positive to Positive Transmission from Current Sub-Matrix.....	17
$\mathbf{E}_j$ Emission from External Source Creating Current.....	18
$\mathbf{T}_{\psi}$ Transmission of Neutrons Due to Flux.....	48
$\mathbf{R}_{\psi}$ Reflection of Neutrons Due to Flux.....	48
$\mathbf{E}_{\psi}$ Emission from External Source Creating Flux.....	48

## List of Abbreviations

Abbreviation	Page
BTE Boltzmann Transport Equation.....	iv
PCT Partial Current Transport.....	iv
SI Source Iteration.....	iv
DD Diamond Difference.....	1
LD Linear Discontinuous.....	1
DI Distribution Iteration.....	3
LN Linear Nodal.....	5
LC Linear Characteristic.....	5
EC Exponential Characteristic.....	9
SC Step Characteristic.....	12
SRD Symmetric Relative Difference.....	29

# IMPROVING LOW ORDER, LINEAR, POSITIVE SPATIAL QUADRATURES FOR THE PARTIAL CURRENT NEUTRON TRANSPORT METHOD

## I. INTRODUCTION

Neutron transport has been a building block of nuclear reaction science since the discovery of fission in the 1930s and 1940s, both for calculations of energy output and for personnel safety. The neutron is the necessary catalyst for nuclear fission and the output of import of both nuclear fission and fusion thereby making the information of where and how many neutrons there are, or neutron flux, a primary interest to nuclear engineers.

Solving the BTE determines the amount of neutron flux. However, the BTE is an integro-differential equation that is not directly solvable except in the simplest cases; therefore it requires a numerical approximation. Discrete Ordinates (deterministic) and Monte Carlo (probabilistic) methods are currently the two major methods for approximating the BTE for neutron transport. Discrete ordinates methods have been popular for approximating the BTE since the early days of nuclear science because of their relative computational ease [1]. For efficiency and simplicity linear methods, such as Diamond Difference (DD) [2], which is 2<sup>nd</sup> order accurate, and Linear Discontinuous (LD) [6], which is 3<sup>rd</sup> order accurate, are widely used. However, unphysical negative fluxes are artifacts of these methods in many common scenarios. Due to these unphysical artifacts discrete ordinates methods are rejected by many (who adopt Monte Carlo methods).

Three competing issues with discrete ordinates methods are linearity, positivity, and accuracy [8]. According to Lathrop, positivity can only be achieved at the cost of accuracy or non-linearity. Depending on the optical thickness and the scattering and absorption properties of the material of the problem, discrete ordinates methods can produce negative fluxes that are

physically nonsensical and computationally time consuming to correct. Spatial distortions, called ray effects, also arise due to the angular quadrature [7], [13]. This leads to the use of more complex methods in order to minimize the amount of negativity [9] or to confine it to regions of low concern. In order to increase the accuracy using a low order, linear method, the spatial mesh must be refined to a point that becomes computationally expensive. Figure 1 is a simple representation of an angular quadrature producing beams or “rays” of neutron flux.

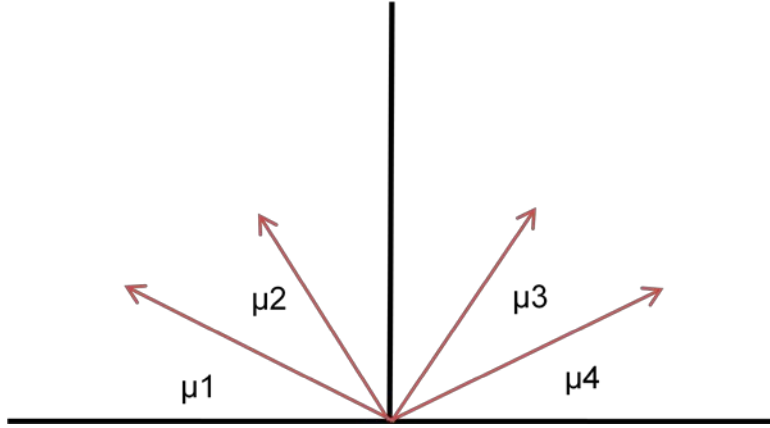


Figure 1: Discrete Ordinates (S4) Representation

In this figure  $\mu_n$  is the cosine of the angle between the direction of the neutron path and the x-axis in slab geometry. The angular quadrature does not produce actual “rays” but represents the number of points used to approximate values on the function, like the number of points that are used to approximate an integral using the Trapezoid Method. The  $S_n$  discretization [1] is the angular quadrature approximation that I use throughout this project, where  $n$  is the number of directions that are used to approximate the BTE for neutron flux. Another concern with this type of angular discretization of the angular flow of neutrons is that when neutrons collide with nuclei there is a continuous distribution of directions into which they can scatter. By only looking at certain direction of neutron flow this limits the accuracy of the approximation. One way to minimize the difference between the approximation and the truth is to increase number of

rays. As the number of directions approaches infinity the approximation approaches the true answer. This is not computationally feasible. However, increasing the number of ordinates will, in theory, bring the approximation closer to the truth.

In recent years many new methods, as well as enhancements to old methods, have been investigated to minimize the negativity and increase the accuracy of the answer. Mathews et al [15] have developed adaptive split-cell characteristic methods of 3<sup>rd</sup> or 4<sup>th</sup> order that preserve positivity. However, these methods, which are non-linear, increase the computational costs, particularly with the new partial-current transport method for  $S_n$  [5].

The Adaptive Partial-Current Discrete Ordinates Radiation Transport with Distribution Iteration (DI) [5], [14], [17], [19] solves many of these problems. However, taking advantage of the linearity of the BTE, attaining the accuracy of the higher order methods, and not introducing the negative fluxes associated with many spatial quadratures requires a method for DI that refines the spatial mesh but does not increase the computational cost. In this research I develop an approach to solve the within-cell transport at negligible extra computational cost for DI using the  $S_n$  angular quadratures using low order, linear, unconditionally positive spatial quadrature methods in a way that achieves the accuracy of higher order methods without the negative flux artifacts of those high order methods. I do this by using creating a very optically thin sub-cell,  $\frac{1}{2^n}$  the thickness of the original cell, where the low order quadratures are very accurate, and then use a merging scheme to combine the cells back to the original cell thickness while retaining the accuracy of the thin sub-cell.

### *I.A. Background*

The issues that have plagued the discrete ordinates methods, negative fluxes and accuracy, have given rise to many attempts to minimize the presence of these



artifacts and to improve the accuracy of the solution. The preferred method of solving the neutron distribution in a material is through the SI method. SI is a Fixed Point Iteration on the neutron source. This method uses a combination of an angular quadrature plus a spatial quadrature, uses a guess for the source, and then walks from one side of the problem, computing the neutron flux in each cell, to the other side of the problem. With the neutron flux, the balance equation can then be solved for the source. The newly computed source is then compared to the original guess. This is repeated until the source is within a given tolerance of the last iteration. As the problem becomes optically thin or the material approaches a pure scattering source, the number of iterations required to achieve a convergence tolerance increases. Thus, attempts to improve discrete ordinates have looked at ways to enhance the SI method.

If the spatial quadratures are limited to low order, linear, and conditionally positive the spatial mesh must be refined. This requires SI to iterate through more cells, slowing the convergence. A method that maintains all three of the desirable qualities has not been developed where the benefits (increase in accuracy) don't outweigh the cost (increase the number of calculations slowing the convergence). Different basis functions for the spatial and angular quadrature have been developed. In this project I do not look in depth at SI, but instead my method improves the performance of PCT with Adaptive DI by improving the fidelity of the spatial model (for a given  $S_n$  model) of transport within each cell.

PCT with Adaptive DI looks at the problem in a different light. Instead of iteratively sweeping through the mesh until the solution converges to an analytic solution, DI solves the within-cell transport by creating a transport matrix for the entire cell that is based on the characteristics of the medium. This matrix describes all the transport, including scatter and emission through the cell. With the internal transport of each cell correct, the inter-cell transport can then be solved using the partial currents at each face. This still requires some iteration, but far fewer in most cases than comparable SI schemes. DI shows promise but

still may fail to perform effectively in some problems, specifically 2-D and 3-D, when spatial quadratures that are not unconditionally positive are used [12]. This leads to the necessity of providing DI with a way to increase the accuracy of positive, linear spatial quadratures to the same level as higher order methods that produce unphysical results.

### *I.A.1 Linearity*

The BTE for neutrons is a linear equation. Therefore any numerical approximation to the linear equation should itself be linear. There are non-linear approximations to the BTE that have been shown to be 3<sup>rd</sup> or 4<sup>th</sup> order accurate. However, these have not been widely accepted because in certain geometries they do not reach the appropriate diffusion limit [11]. Also, because these quadratures are non-linear, after each iteration, some parameters of the method change because the flux changes, so all the spatial quadrature coefficients must be recalculated and new matrices (for DI) are needed and are different in every cell. This is disastrous in both storage (RAM) and time. Therefore, methods that are linear (i.e. DD, LD, Linear Nodal (LN), and Linear Characteristic (LC)) are more accepted and generally more desirable.

### *I.A.2 Positivity*

As pointed out by Lathrop [8] the primary trade off for discrete ordinates methods comes in part due to the physical requirement of the solution (i.e. the neutron flux, or dose) to be positive. Negative fluxes arise because of a) Too thick cells when using conditionally positive spatial quadratures (e.g. DD in slab geometry), b) Discontinuous boundary conditions with 2-D or 3-D and methods with negative coefficients (e.g. DD on rectangles), and c) Truncated Spherical Harmonics / Legendre expansions of anisotropic scatter combined with an unfortunate choice of angular quadrature set. Many scientists and engineers will not blithely accept the condition that there is a negative flux of neutrons on the

basis that the negative flux in question is present in only a portion of the solution space. This casts serious doubts onto the validity of the method as a whole. The fix-ups that have been developed look for negative fluxes and then adapt the method to that space, forcing the solution to zero or a positive value, then rebalance the equation. By rebalancing the equation, the fix up ensures particle conservation, but it also reduces the method to 1<sup>st</sup> order accuracy wherever the fix up is applied.

### *I.A.3 Accuracy*

The final issue of importance for discrete ordinates methods is that of accuracy. Again pointing to Lathrop's discussion of the tradeoff between positivity and accuracy, the 2<sup>nd</sup> order and higher methods that are linear are at best only conditionally positive. DD is not even conditionally positive in 2-D and 3-D. The fix-ups that have been employed to overcome the negativity in some quadrature methods are generally only 1<sup>st</sup> order accurate. By using these fix-ups the accuracy gained by the higher order conditionally positive methods are negated by the low order of the fix-up. This shows that of the three desirable characteristics of discrete ordinates methods, it is possible to have only two out of three. You can have high order accuracy and positivity, but not linearity. Or you can choose high order accuracy and linearity, but not guarantee positivity. And finally, you can have linearity and positivity, but attain only 1<sup>st</sup> order accuracy.

### *I.A.4 Distribution Iteration*

DI was developed by Mathews, Prins, Wager, and Dishaw [5],[14], [17], [19], with the idea that the within-cell transport could be represented by a set of coefficient matrices that act on the incoming flux and contain within them all the information regarding the transmission, reflection, scattering and escape of neutrons through, within, and out of the medium. The matrices are set up using

a set of balance equations dependant on the properties of the medium, thickness of the cell, and the spatial quadrature that is being used. The matrices can be set up once and then they do not change for that medium. In this project I will use the  $S_n$  angular quadrature set to approximate the BTE within each cell. For example, Figure 1 shows an  $S_4$  representation, in which there are four discrete angles,  $\mu_1$ ,  $\mu_2$ ,  $\mu_3$ , and  $\mu_4$ .

### *I.B. Motivation*

A method needs to be developed that enables a linear, positive spatial quadrature, that is low order accurate to attain the accuracy of the higher order quadratures that violate linearity or positivity. This will bypass the possible failures that may arise in DI from quadratures that are non-linear or that produce negative neutron flux.

### *I.C. Objectives*

The objectives of this research are to: 1) increase the accuracy of positive, linear spatial quadratures to that of higher order methods, 2) maintain numerical stability in the matrices that it produces, and 3) produce a method that can be integrated into existing DI codes.

1. *Increased Accuracy:* Based on the desire to have a linear and positive spatial quadrature, and due to the fact that such methods are only 1<sup>st</sup> order accurate, this is the key objective of this project. The results will be compared to a benchmark to validate that the method can produce similar accuracy of higher order methods. This method will be compared to a benchmark (SI) code that has been developed and improved over the last 15 years [18]. This will insure that this method can achieve the accuracy of higher order methods.

2. *Numerical Stability:* In order for this method to reach the accuracy of higher order methods, matrix inversions are required to emulate the mesh

refinement required by SI methods. This will require that the matrices be well-conditioned.

3. *Integration into DI Code:* Upon successful testing, my method will produce the matrices that are used in slab geometry by DI codes. This method will improve the performance of 1<sup>st</sup> order, linear, positive spatial quadratures in the existing DI codes.

### *I.D. Statement of the Problem*

Develop a method that can be incorporated into existing slab geometry DI codes that implements linear, unconditionally positive, hence only 1<sup>st</sup> order accurate, spatial quadratures for the discrete ordinates approximation to the BTE that achieves the accuracy of high order methods that are not positive or not linear.

### *I.E. Scope and Limitations*

Method:

1-D Cartesian (Slab) geometry

1 Energy group

Testing:

Subcritical steady state (not eigenvalue problems)

$C < 1$

Demonstrate Step and SC, benchmarking each against SI

Compare to DD and EC

### *I.F. Approach*

The first step is to set up the equations for the partial currents and fluxes for the original-sized cell based on the spatial and angular quadratures. Once the cells are split the next step is to solve the simultaneous equations for the two cells in order to eliminate the currents and fluxes between the two adjacent cells, thus combining the two smaller cells into a cell twice as big. This gives the

equations for the combined cells, and is repeated until the sub-cells are combined to the original-sized cell.

The next step is to use the Step and SC spatial quadratures (linear, positive, and 1<sup>st</sup> order) and test and verify the currents and fluxes produced by this method against the same quadratures using an SI code.

Finally the method is compared to a benchmark (Exponential Characteristic (EC) in the SI code) in several different problem scenarios to show that the low order, positive, linear spatial quadratures can provide the accuracy of the higher order method. The problem scenarios use characteristics of cell width (based on the mean free path of the neutrons in the given material), scattering ratios, internal neutron source, and external neutron illumination to compute the partial currents out each face of the original cell and the average scalar flux in the cell.

## II. THEORY

As all discrete ordinates methods, and neutron transport theory in general, the object of the approximation is to find the flux of neutrons at a particular location or throughout the space of interest. The BTE is the basis for all neutron transport and in its full form describes the motion of neutrons based on their energy, location, and the scattering and absorption properties of the material through which they are moving. Without making any simplifying assumptions regarding energies or discretizing space and angle we assume the BTE for neutron transport to be:

$$\left[\frac{1}{v} \frac{\partial}{\partial t} + \hat{\Omega} \cdot \nabla + \sigma(\vec{r}, E, t)\right] \psi(\vec{r}, \hat{\Omega}, E, t) = q(\vec{r}, \hat{\Omega}, E, t). \quad (1)$$

For this work the BTE has been reduced, in discrete ordinates, to a time-independent, mono-energetic cell balance equation in the following form:

$$j^{out} + \sigma \Delta x \psi_A = \sigma_s \varphi \Delta x + S^{ext} \Delta x + j^{in}, \quad (2)$$

where  $\sigma$  is the total cross section of the material,  $\sigma_s$  is the scattering cross section and  $\Delta x$  is the thickness of the cell. Figure 2 is a representation of a cell with the transport of neutrons into, through and out of the cell in all directions ( $\mu$ ), and where:

$$j^{in}(\mu) = \begin{cases} \mu \psi_L(\mu) & \mu \geq 0, \\ -\mu \psi_L(\mu) & \mu < 0, \end{cases} \quad (3)$$

$\psi_L(\mu)$  is the flux at the left side of the cell;  $\psi_R(\mu)$  is the flux at the right side of the cell;  $\psi_A(\mu)$  is the average flux in the cell (spatially averaged);  $S^{ext}(\mu)$  is the emission source inside the cell, assumed to be spatially uniform and isotropic; and

$\varphi_A = \int_{-1}^1 \psi_A(\mu) d\mu$  is the average scalar flux in the cell.

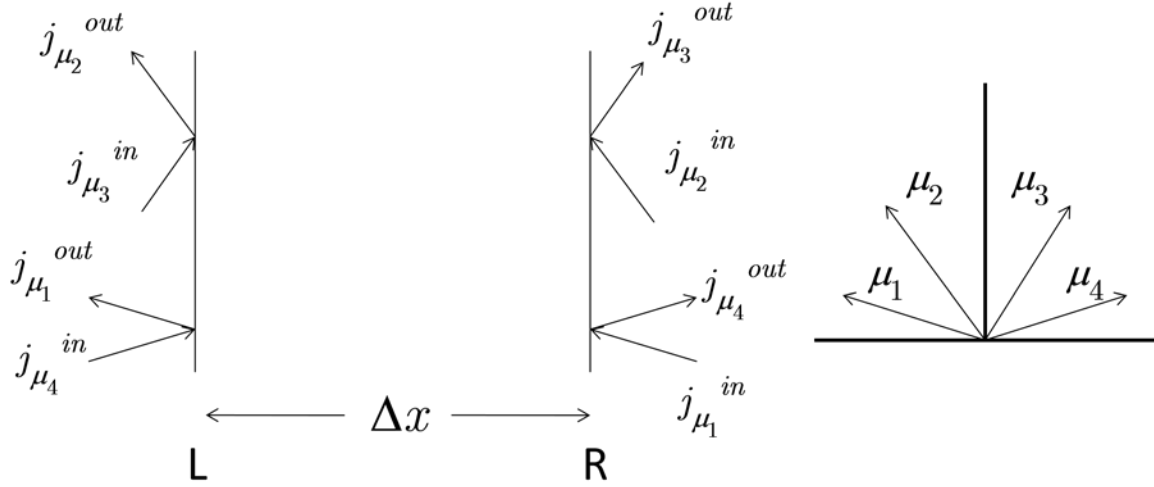


Figure 2: Within-Cell Transport

Neutron transport does not include anti-neutrons or neutron holes (unlike electron transport in transistors), so the actual flux is non-negative:

$$\psi(x, \mu) \geq 0. \quad (4)$$

A numerical method that ensures that its solutions have this property is said to be a positive method. In discrete ordinates calculations, most spatial quadrature methods are not positive.

### II.A. Angular Quadratures

There are many ways to discretize the angular space of neutron transport problems. For this project I use the  $S_n$ , or discrete ordinates, angular quadrature approximations, specifically the single-range Gauss-Legendre angular quadrature sets in slab. See, for example, Lewis and Miller [7]. The approximation approaches the analytical solution to the transport equation as the number of ordinates approaches infinity. This is not computationally possible. Although I explored the performance of my methods using  $S_2$  through  $S_8$ , the testing reported here used  $S_8$ , being the most challenging of these.



## II.B. Spatial Quadratures

As the problem statement declares, the crux of the problem is to develop a method that allows a low order spatial quadrature that is linear and unconditionally positive to achieve the accuracy of a high-order quadrature that may be either linear or positive, but not both. While many spatial quadratures have been proposed, I used four spatial quadratures in this work: DD, Step, Step Characteristic (SC), and EC. Table 1 summarizes the four spatial quadratures on which I focus.

Table 1: Spatial Quadrature Comparison

Name	Abbreviation	Order*	Positivity	Linearity	Description
Step	ST	1	X	X	Constant discontinuous flux approx.
Step Characteristic	SC	1	X	X	Constant discontinuous scattering source approx
Diamond Difference	DD	2		X	Divided difference approx.
Exponential Characteristic	EC	4	X		

\* error proportional to

$$(\sigma_{\Delta x})^n$$

Of the low-order methods, DD is the most accurate, having second order accuracy, but is only conditionally positive. The condition that gives DD the negativity is the thickness of the cell in which it is used. This condition takes the DD method out of consideration for this method. Interestingly, even though DD has this conditional positivity, it is still the preferred choice of some members of the transport community.

Exponential Characteristic is a method that was developed for slab geometry at the Air Force Institute of Technology [15]. This method uses a characteristic integration of the Boltzmann transport equation with an exponential function as the assumed form of the source distribution, continuous across each spatial cell.

This leaves two methods, both of which are only first order accurate, but are both unconditionally positive, Step and Step Characteristic (SC). Step is a linear discontinuous approximation. The Step approximation is similar to a backward Euler approximation. Step makes the auxiliary assumption that the average flux in the cell is constant and continuous at the outflow of the cell but discontinuous at the inflow of the cell. SC makes a similar assumption of a constant scattering source that is that is continuous at the outflow of the cell but discontinuous at the inflow of the cell. Of these two methods step is the most straightforward, but neither one is complicated or expensive to calculate. Based on this summary of quadratures and being consistent with the objectives of this project, it is clear that the only spatial quadratures, of the four examined here, that meet the criteria are Step and SC.

### *II.C. Within-Cell Transport*

The within-cell transport problem is at the heart of the PCT method: It solves the within-cell transport and collapses that into a global partial current that is used to determine the partial currents out of each face of a cell based upon the partial currents into each face of the cell and the internal source.

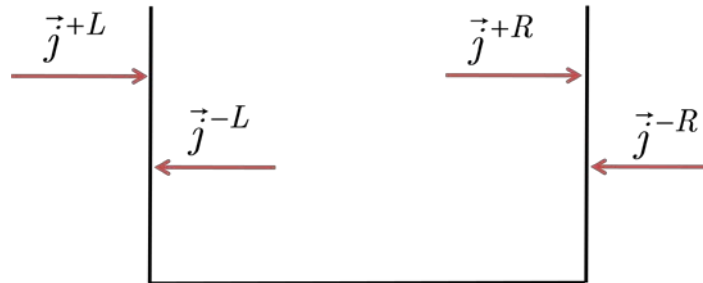


Figure 3: One Cell Currents

#### *II.C.1 Calculating the Within-Cell Transport Matrices*

While much of the following equations were developed for DI by Mathews and Dishaw [5], [14], they are critical to this project. Therefore, an explanation of the terms and algebraic manipulation of the matrices involved is advantageous. The solution to the method can be observed as either the currents coming out of the cell or as the average flux in the cell. Because the flux in the cell generated a scattering source which in turn creates a flux or current the two systems are closely related. I will develop both of the system of equations as they relate to this method. The basic algorithm for determining the currents out of each of the cell faces and the average flux in the cell is as follows:

Starting with one cell as in Figure 2, where, for  $S_4$  (with  $-1 < \mu_1 < \dots < \mu_4 < 1$ )

$$\vec{j}^{out} = \begin{pmatrix} j_{\mu 1}^L \\ j_{\mu 2}^L \\ j_{\mu 3}^R \\ j_{\mu 4}^R \end{pmatrix} \quad (5)$$

and

$$\vec{j}^{in} = \begin{pmatrix} j_{\mu 1}^R \\ j_{\mu 2}^R \\ j_{\mu 3}^L \\ j_{\mu 4}^L \end{pmatrix} \quad (6)$$

The average flux in the cell can be represented as

$$\psi = \mathbf{K}^{\psi, in} \vec{j}^{in} + \mathbf{K}^{\psi, E} \vec{S}^{ext} + \mathbf{K}^{\psi, S} \mathbf{S}^S, \quad (7)$$

where  $\psi$  is the average flux in the cell,  $S^{ext}$  is the source due to external emission within the cell, and  $S^S$  is the source due to scattering within the cell, all of which are vectors of size  $n$  ( $S_n$ ), based on the angular quadrature used.  $\mathbf{K}^{\psi, in}$  represents the flux, approximated by a specific spatial quadrature, that is due to current in. Likewise,  $\mathbf{K}^{\psi, E}$  and  $\mathbf{K}^{\psi, S}$  represent the flux due to the external

source, and the flux from the scatter within the cell, respectively. The  $\mathbf{K}$  matrices, developed in Appendices A and B for Step and SC, respectively, are square, diagonal matrices ( $n \times n$ ).

The scatter source is a scattering matrix that operates on the flux

$$\mathbf{S}^S = \Sigma^{S,\psi} \psi \quad (8)$$

Substituting (8) into (7) gives the flux in terms of itself,

$$\psi = \mathbf{K}^{\psi,in} \vec{\mathbf{j}}^{in} + \mathbf{K}^{\psi,E} \vec{\mathbf{S}}^{ext} + \mathbf{K}^{\psi,S} \Sigma^{S,\psi} \psi, \quad (9)$$

Solving for  $\psi$  using matrix notation gives

$$\mathbf{I}\psi - \mathbf{K}^{\psi,S} \Sigma^{S,\psi} \psi = \mathbf{K}^{\psi,in} \vec{\mathbf{j}}^{in} + \mathbf{K}^{\psi,E} \vec{\mathbf{S}}^{ext}, \quad (10)$$

$$\psi = (\mathbf{I} - \mathbf{K}^{\psi,S} \Sigma^{S,\psi})^{-1} (\mathbf{K}^{\psi,in} \vec{\mathbf{j}}^{in} + \mathbf{K}^{\psi,E} \vec{\mathbf{S}}^{ext}), \quad (11)$$

The inverse operator in this equation accounts for all scatters that occur throughout the cell. Let

$$\mathbf{L} = (\mathbf{I} - \mathbf{K}^{\psi,S} \Sigma^{S,\psi})^{-1}, \quad (12)$$

So that

$$\psi = \mathbf{L} \mathbf{K}^{\psi,in} \vec{\mathbf{j}}^{in} + \mathbf{L} \mathbf{K}^{\psi,E} \vec{\mathbf{S}}^{ext}. \quad (13)$$

Now the flux that is generated by the external source and the flux that is generated directly from current coming into the cell can be separated. This gives  $\mathbf{m}$  matrices for the flux

$$\mathbf{m}^{\psi,in} = \mathbf{L} \mathbf{K}^{\psi,in} \quad (14)$$

and

$$\mathbf{m}^{\psi,ext} = \mathbf{L} \mathbf{K}^{\psi,E}. \quad (15)$$

Substituting (14) and (15) into (13) gives the solution for the flux in the cell from current coming into the cell and external emission source:

$$\psi = \mathbf{m}^{\psi,in} \vec{\mathbf{j}}^{in} + \mathbf{m}^{\psi,ext} \vec{\mathbf{S}}^{ext} \quad (16)$$

Looking at the contributions to currents out of the cell that come from all sources is similar to the contributions to the flux:

$$\vec{\mathbf{j}}^{out} = \mathbf{K}^{O,in} \vec{\mathbf{j}}^{in} + \mathbf{K}^{O,E} \vec{\mathbf{S}}^{ext} + \mathbf{K}^{O,S} \mathbf{S}^S. \quad (17)$$

Substituting (8) in to (17) gives

$$\vec{\mathbf{j}}^{out} = \mathbf{K}^{O,I} \vec{\mathbf{j}}^{in} + \mathbf{K}^{O,E} \vec{\mathbf{S}}^{ext} + \mathbf{K}^{O,S} \Sigma^{S,\psi} \Psi. \quad (18)$$

Now by substituting (13) into (18) gives the total current out of the cell based current into the cell, current from the external source and the current from the scatters:

$$\vec{\mathbf{j}}^{out} = \mathbf{K}^{O,in} \vec{\mathbf{j}}^{in} + \mathbf{K}^{O,E} \vec{\mathbf{S}}^{ext} + \mathbf{K}^{O,S} \Sigma^{S,\psi} (\mathbf{L} \mathbf{K}^{\psi,in} \vec{\mathbf{j}}^{in} + \mathbf{L} \mathbf{K}^{\psi,E} \vec{\mathbf{S}}^{ext}). \quad (19)$$

Expanding and rearranging (19) gives

$$\vec{\mathbf{j}}^{out} = (\mathbf{K}^{O,in} + \mathbf{K}^{O,S} \Sigma^{S,\psi} \mathbf{L} \mathbf{K}^{\psi,in}) \vec{\mathbf{j}}^{in} + (\mathbf{K}^{O,E} + \mathbf{K}^{O,S} \Sigma^{S,\psi} \mathbf{L} \mathbf{K}^{\psi,E}) \vec{\mathbf{S}}^{ext} \quad (20)$$

Collecting the terms that act on  $\vec{\mathbf{j}}^{in}$  and  $\vec{\mathbf{S}}^{ext}$  gives the  $\mathbf{m}$  matrices that act on  $\vec{\mathbf{j}}^{in}$  and  $\vec{\mathbf{S}}^{ext}$  in order to produce

$$\vec{\mathbf{j}}^{out} = \mathbf{m}^{out,in} \vec{\mathbf{j}}^{in} + \mathbf{m}^{out,ext} \vec{\mathbf{S}}^{ext} \quad (21)$$

where the matrix of coefficients that acts directly on  $\vec{\mathbf{j}}^{in}$  represent the  $\mathbf{m}^{out,in}$ :

$$\mathbf{m}^{out,in} = \mathbf{K}^{O,in} + \mathbf{K}^{O,S} \Sigma^{S,\psi} \mathbf{L} \mathbf{K}^{\psi,in} \quad (22)$$

and the matrix of coefficients that act on the external emission source and source produce by scattering is:

$$\mathbf{m}^{out,ext} = \mathbf{K}^{O,E} + \mathbf{K}^{O,S} \Sigma^{S,\psi} \mathbf{L} \mathbf{K}^{\psi,E} \quad (23)$$

The  $\mathbf{m}$  matrices can also be represented as the transmittance and reflectance of the neutrons that pass through the cell in the case of  $\vec{\mathbf{j}}^{in}$ , or the escape of neutrons that are emitted in the cell in the case of  $\vec{\mathbf{S}}^{ext}$ , producing either current out of the cell through each of the cell faces, to include any scattering that may happen, or the average flux in the cell. The  $\mathbf{m}$  matrices for the currents out of the cell are

$$\mathbf{m}^{out,in} = \begin{pmatrix} \mathbf{T}_j^{--} & \mathbf{R}_j^{-+} \\ \mathbf{R}_j^{+-} & \mathbf{T}_j^{++} \end{pmatrix} \quad (24)$$

and

$$\mathbf{m}^{out,ext} = \begin{pmatrix} \mathbf{E}_j^{--} & \mathbf{E}_j^{-+} \\ \mathbf{E}_j^{+-} & \mathbf{E}_j^{++} \end{pmatrix}. \quad (25)$$

In these matrices the superscripts indicate the final direction of flow followed by the initial direction of flow and the subscripts specify the source of the flow, either from current,  $j$ , or flux,  $\psi$ .  $\mathbf{T}$  corresponds to a transmission of neutrons through the cell,  $\mathbf{R}$  to a reflection in a cell, and  $\mathbf{E}$  to the emission of neutrons from the external source,  $S^{ext}$ . For example,  $\mathbf{T}_\psi^{-+}$  is the transmission of neutrons from flux that was initially going in the positive direction but after some number of scatters is now going in the negative direction.

In equation (24)  $\mathbf{T}_j^{--}$  the transmission of  $j^{in}$  that enters the cell through the right boundary, moving in the negative  $x$  direction (one of the negative  $\mu$  ordinates), is scattered zero or more times, and exits through the left boundary in the negative direction (continuing in one of the negative  $\mu$  ordinates).  $\mathbf{R}_j^{-+}$  is the reflection of  $j^{in}$  that enters the cell at the left boundary moving in the positive  $x$  direction (one of the positive  $\mu$  ordinates), is scattered one to many times and leaves through the left boundary moving in the negative  $x$  direction (one of the negative  $\mu$  ordinates). Similarly,  $\mathbf{R}_j^{+-}$  is the reflection of  $j^{in}$  that enters in at the right boundary moving in the negative direction (one of the negative  $\mu$  ordinates), scatter one to many times and leaves the cell through the right boundary moving in the positive  $x$  direction (one of the positive  $\mu$  ordinates). Finally,  $\mathbf{T}_j^{++}$  is the transmittance of  $j^{in}$  through the cell with zero or more scatters, entering the cell through the left boundary moving in the positive  $x$  direction (one of the positive  $\mu$  ordinates) and leaving the cell through

the right boundary continuing in the positive x direction (continuing in one of the positive  $\mu$  ordinates). I have used the  $\mathbf{m}^{out,in}$  matrix as an example.

However, the other matrices,  $\mathbf{m}^{out,ext}$ ,  $\mathbf{m}^{\psi,in}$ , and  $\mathbf{m}^{\psi,ext}$ , are similar.

Special care must be taken to ensure that the correct sub-matrices,  $\mathbf{T}$ ,  $\mathbf{R}$ , and  $\mathbf{E}$ , are used in these equations because they are unique. This complicates the algebra but once the system is set up it can be repeated easily. Substituting the sub-matrices for the  $\mathbf{m}$  matrices, we can now represent the current as follows:

$$\mathbf{j}^{-L} = \mathbf{T}_j^{--} \vec{\mathbf{j}}^{-R} + \mathbf{R}_j^{-+} \vec{\mathbf{j}}^{+L} + \mathbf{E}_j^{--} \vec{\mathbf{S}}^{ext,-} + \mathbf{E}_j^{-+} \vec{\mathbf{S}}^{ext,+} \quad (26)$$

$$\vec{\mathbf{j}}^{+R} = \mathbf{R}_j^{+-} \vec{\mathbf{j}}^{-R} + \mathbf{T}_j^{++} \vec{\mathbf{j}}^{+L} + \mathbf{E}_j^{+-} \vec{\mathbf{S}}^{ext,-} + \mathbf{E}_j^{++} \vec{\mathbf{S}}^{ext,+} \quad (27)$$

where now each of the  $\vec{\mathbf{j}}$  and  $\vec{\mathbf{S}}^{ext}$  vectors is of length  $n/2$  and sub-matrices are of size  $(n/2 \times n/2)$ .

The flux can also be broken down into it individual sub-matrices acting on the current into the cell and the external emission source:

$$\psi^- = \mathbf{T}_\psi^{--} \vec{\mathbf{j}}^{-R} + \mathbf{R}_\psi^{-+} \vec{\mathbf{j}}^{+L} + \mathbf{E}_\psi^{--} \vec{\mathbf{S}}^{ext,-} + \mathbf{E}_\psi^{-+} \vec{\mathbf{S}}^{ext,+} \quad (28)$$

$$\psi^+ = \mathbf{R}_\psi^{+-} \vec{\mathbf{j}}^{-R} + \mathbf{T}_\psi^{++} \vec{\mathbf{j}}^{+L} + \mathbf{E}_\psi^{+-} \vec{\mathbf{S}}^{ext,-} + \mathbf{E}_\psi^{++} \vec{\mathbf{S}}^{ext,+} \quad (29)$$

Algorithm 1 is the basic process that DI uses to solve the partial currents. This is done on a fixed size cell which only allows the spatial quadrature to attain the accuracy for that optical thickness. My method of merging optically thin cells, demonstrated in the next section, can be used by DI to solve the same problem but allows the first-order, positive spatial quadratures to achieve a much higher accuracy.

---

**Algorithm 1: Basic Conceptual Algorithm**

---

Initialize:

1. Use problem data and the choice of basis functions to generate the  $\mathbf{K}$  matrices.
  2. Solve for the cell  $\mathbf{m}$  matrix.
  3. Use emission sources and within-cell transport to evaluate outflow currents due to emission sources
  4. Initialize the inflow current distributions (e.g. uniform and isotropic)
  5. Solve for the partial currents out each face and average flux within the cell
- 

### *II.C.2 Merging Cells*

The previous section characterizes the transport of neutrons, in an angular discretization of the cell, based on an arbitrary spatial quadrature, through one cell. The accuracy of the computations is implicit in the  $\mathbf{K}$  matrices that are dependent upon cell thickness,  $\Delta x$ . As discussed in the background section, in order for a linear and positive spatial quadrature to attain high accuracy the cell must be sub-divided until it is optically thin, in order for the first-order, positive, linear methods to be accurate. In the SI method, this is done by refining the mesh and sweeping through more cells. However, as pointed out, this slows the computation time and when extended to 2- and 3-D geometries, increases the cost of the calculation faster than the benefits. As will be shown this project will produce a method that calculates the  $\mathbf{m}$  matrices for the smallest sub-divided cell and merges them matrices back to the original size cell.

A simple illustration, shown in Figures 4 through 11, will assist in understanding the method. Using  $n = 3$  the original cell is divided into  $2^3$  (8) sub-cells:



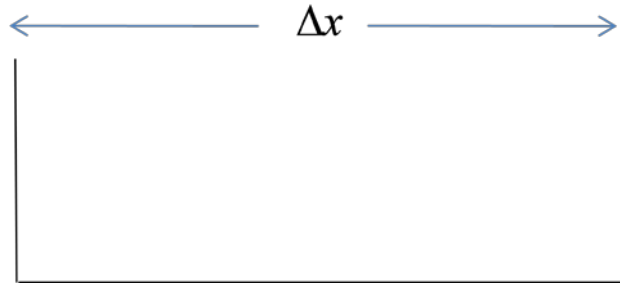


Figure 4: Original Cell

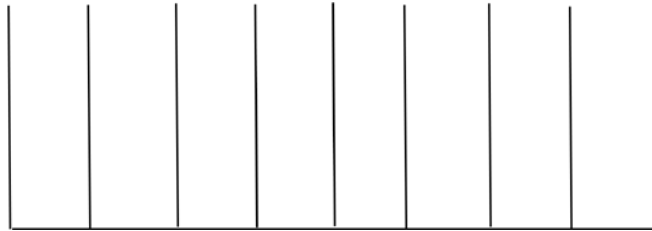


Figure 5: Cell Divided into Smallest Sub-cells

DO I = n, 1, -1

i = 3: Merge two of the smallest sub-cells

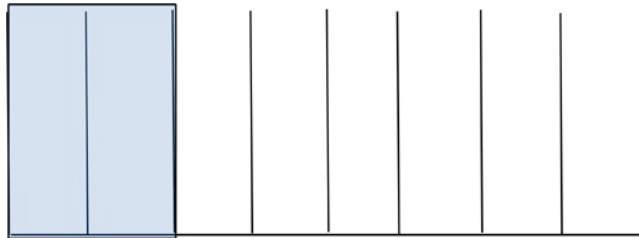


Figure 6: Merge #1

Rearrange terms and collect **T**, **R**, and **E** sub-matrices into new **m** matrices. This now represents a set of sub-cells twice as big.

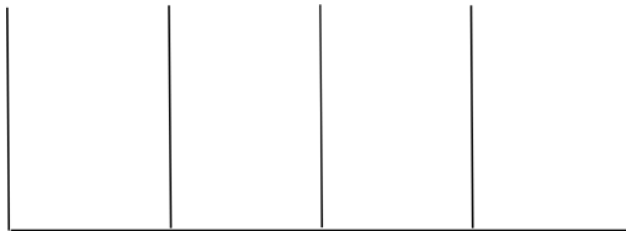


Figure 7: Merge 1 Result

$n = 2$ : Merge two of the smallest sub-cells

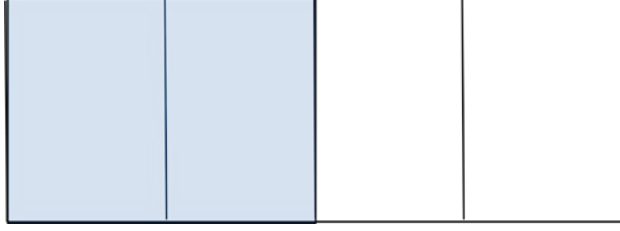


Figure 8: Merge #2

Rearrange terms and collect  $\mathbf{T}$ ,  $\mathbf{R}$ , and  $\mathbf{E}$  sub-matrices into new  $\mathbf{m}$  matrices.

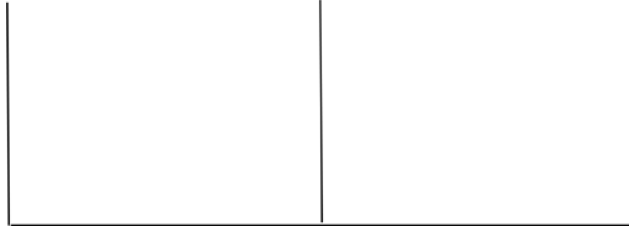


Figure 9: Merge 2 Result

$n = 1$ : Merge two of the smallest sub-cells

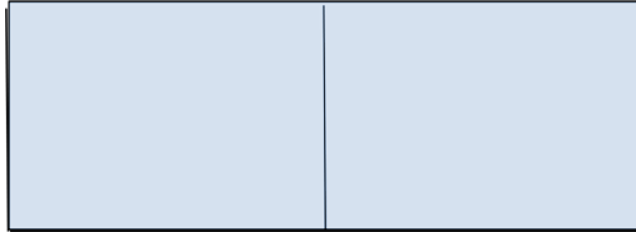


Figure 10: Merge #3

$n = 0$ : Rearrange terms and collect  $\mathbf{T}$ ,  $\mathbf{R}$ , and  $\mathbf{E}$  sub-matrices into new  $\mathbf{m}$  matrices.

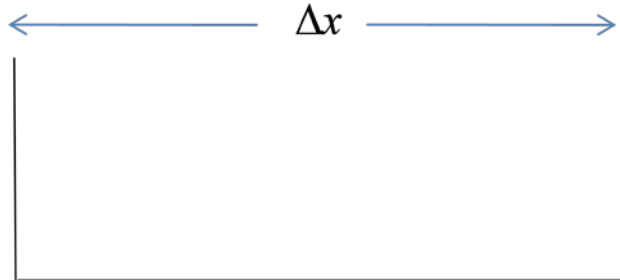


Figure 11: Merge 3 Result

Comparing Figure 11 to Figure 4, after 3 merges the cell is back to its original thickness. However, it now has the same accuracy for the solution to the current out and the flux in the original cell as if it was  $1/8^{\text{th}}$  the thickness. On a scale of  $2^3$  this does not appear to be that important. However, if the thickness required for accuracy is  $2^{10}$ , SI will be required to compute the current and flux through 1,024 sub-cells, whereas the method for DI will compute only 10 merges and merges are only done once for one cell of a specific size and composition (material). It will be shown later that using Step in SI for a particular problem required  $2^{19}$  (524,288) sub-cells in order to attain the same accuracy as using EC in SI. For this method that requires only 19 merges, this constitutes a savings of computation time of many orders of magnitude.

Using my method I am able to accomplish this without an expensive increase in the computation time, since all of these calculations are done once at the beginning of the problem and instead of having to sweep through  $2^n$  sub-cells, as in SI, my method only has to calculate  $n$  merges in order to achieve the same level of accuracy.

### *II.C.2.1 The Merging Process*

Figure 12 shows simple example of dividing the original cell into two equal cells of half the original size. Even though the picture is simple the algebraic manipulation of the matrices is not. In this section I will explain each step of the merging process of two identical sub-cells that can be done repeatedly until the cell is back to the original thickness.

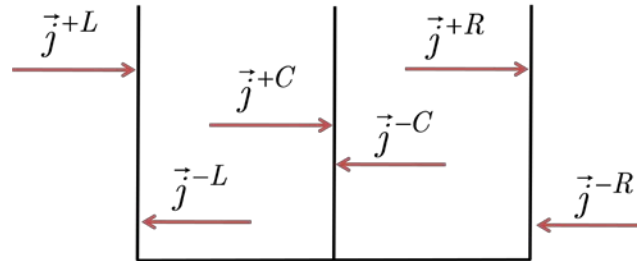


Figure 12: Currents in Split Cells

Using the same scheme as before, the  $\mathbf{m}$  matrices can be formed for the smallest sub-cell. Since this cell is comprised of the same material as before the computation of the K and m matrices can be done using the same algorithm. Using Figure 11 as an example, where  $n = 1$ , the current out of this new system of cells can be represented the same as in (26) and (27).

$$\mathbf{j}^{-L} = \mathbf{T}_j^{--}\bar{\mathbf{j}}^{-C} + \mathbf{R}_j^{-+}\bar{\mathbf{j}}^{+L} + \mathbf{E}_j^{--}\bar{\mathbf{S}}^{ext,-} + \mathbf{E}_j^{-+}\bar{\mathbf{S}}^{ext,+} \quad (30)$$

$$\bar{\mathbf{j}}^{+C} = \mathbf{R}_j^{+-}\bar{\mathbf{j}}^{-C} + \mathbf{T}_j^{++}\bar{\mathbf{j}}^{+L} + \mathbf{E}_j^{+-}\bar{\mathbf{S}}^{ext,-} + \mathbf{E}_j^{++}\bar{\mathbf{S}}^{ext,+} \quad (31)$$

$$\mathbf{j}^{-C} = \mathbf{T}_j^{--}\bar{\mathbf{j}}^{-R} + \mathbf{R}_j^{-+}\bar{\mathbf{j}}^{+C} + \mathbf{E}_j^{--}\bar{\mathbf{S}}^{ext,-} + \mathbf{E}_j^{-+}\bar{\mathbf{S}}^{ext,+} \quad (32)$$

$$\bar{\mathbf{j}}^{+R} = \mathbf{R}_j^{+-}\bar{\mathbf{j}}^{-R} + \mathbf{T}_j^{++}\bar{\mathbf{j}}^{+C} + \mathbf{E}_j^{+-}\bar{\mathbf{S}}^{ext,-} + \mathbf{E}_j^{++}\bar{\mathbf{S}}^{ext,+} \quad (33)$$

Because the material is the same for both of the sub-cells, the external emission source does not need to have a subscript in order to define which cell it is in.

Both of the sources are the same.

In order to merge the two sub-cells, the currents at the center face must be eliminated. This is done through a series of linear algebra equations. In this section I will focus on the merging of the matrices resulting in current only. The merging of matrices for the flux is presented in Appendix C

Substituting (32) into (31) and solving for  $\mathbf{j}^{+C}$  we get:

$$\begin{aligned} \bar{\mathbf{j}}^{+C} = & \mathbf{R}_j^{+-}(\mathbf{T}_j^{--}\bar{\mathbf{j}}^{-R} + \mathbf{R}_j^{-+}\bar{\mathbf{j}}^{+C} + \mathbf{E}_j^{--}\bar{\mathbf{S}}^{ext,-} + \mathbf{E}_j^{-+}\bar{\mathbf{S}}^{ext,+}) \\ & + \mathbf{T}_j^{++}\bar{\mathbf{j}}^{+L} + \mathbf{E}_j^{+-}\bar{\mathbf{S}}^{ext,-} + \mathbf{E}_j^{++}\bar{\mathbf{S}}^{ext,+} \end{aligned} \quad (34)$$

$$\begin{aligned} \bar{\mathbf{j}}^{+C} = & (\mathbf{I} - \mathbf{R}_j^{+-}\mathbf{R}_j^{-+})^{-1}(\mathbf{R}_j^{+-}\mathbf{T}_j^{--}\bar{\mathbf{j}}^{-R} + \mathbf{R}_j^{+-}\mathbf{E}_j^{--}\bar{\mathbf{S}}^{ext,-} \\ & + \mathbf{R}_{o,i}^{+-}\mathbf{E}_j^{-+}\bar{\mathbf{S}}^{ext,+} \\ & + \mathbf{T}_j^{++}\bar{\mathbf{j}}^{+L} + \mathbf{E}_j^{+-}\bar{\mathbf{S}}^{ext,-} + \mathbf{E}_j^{++}\bar{\mathbf{S}}^{ext,+}) \end{aligned} \quad (35)$$

Similarly, substituting (31) into (32) and solving for  $\mathbf{j}^{-C}$  we get:

$$\mathbf{j}^{-C} = \mathbf{T}_j^{--} \bar{\mathbf{j}}^{-R} + \mathbf{R}_j^{-+} (\mathbf{R}_j^{+-} \bar{\mathbf{j}}^{-C} + \mathbf{T}_j^{++} \bar{\mathbf{j}}^{+L} + \mathbf{E}_j^{+-} \bar{\mathbf{S}}^{ext,-} + \mathbf{E}_j^{++} \bar{\mathbf{S}}^{ext,+}) + \mathbf{E}_j^{--} \bar{\mathbf{S}}^{ext,-} + \mathbf{E}_j^{-+} \bar{\mathbf{S}}^{ext,+} \quad (36)$$

$$\mathbf{j}^{-C} = (\mathbf{I} - \mathbf{R}_j^{-+} \mathbf{R}_j^{+-})^{-1} (\mathbf{T}_j^{--} \bar{\mathbf{j}}^{-R} + \mathbf{R}_j^{-+} \mathbf{T}_j^{++} \bar{\mathbf{j}}^{+L} + \mathbf{R}_j^{-+} \mathbf{E}_j^{+-} \bar{\mathbf{S}}^{ext,-} + \mathbf{R}_j^{-+} \mathbf{E}_j^{++} \bar{\mathbf{S}}^{ext,+} + \mathbf{E}_j^{--} \bar{\mathbf{S}}^{ext,-} + \mathbf{E}_j^{-+} \bar{\mathbf{S}}^{ext,+}) \quad (37)$$

Substituting (37) into (30) we get the current out the left side of the cell:

$$\mathbf{j}^{-L} = \mathbf{T}_j^{--} ((\mathbf{I} - \mathbf{R}_j^{-+} \mathbf{R}_j^{+-})^{-1} (\mathbf{T}_j^{--} \bar{\mathbf{j}}^{-R} + \mathbf{R}_j^{-+} \mathbf{T}_j^{++} \bar{\mathbf{j}}^{+L} + \mathbf{R}_j^{-+} \mathbf{E}_j^{+-} \bar{\mathbf{S}}^{ext,-} + \mathbf{R}_j^{-+} \mathbf{E}_j^{++} \bar{\mathbf{S}}^{ext,+} + \mathbf{E}_j^{--} \bar{\mathbf{S}}^{ext,-} + \mathbf{E}_j^{-+} \bar{\mathbf{S}}^{ext,+})) + \mathbf{R}_j^{--} \bar{\mathbf{j}}^{+L} + \mathbf{E}_j^{--} \bar{\mathbf{S}}^{ext,-} + \mathbf{E}_j^{-+} \bar{\mathbf{S}}^{ext,+} \quad (38)$$

Likewise, substituting (35) into (33) we get the current out of the right side of the cell:

$$\begin{aligned} \bar{\mathbf{j}}^{+R} = & \mathbf{R}_j^{+-} \bar{\mathbf{j}}^{-R} + \mathbf{T}_j^{++} ((\mathbf{I} - \mathbf{R}_j^{+-} \mathbf{R}_j^{-+})^{-1} (\mathbf{R}_j^{+-} \mathbf{T}_j^{--} \bar{\mathbf{j}}^{-R} + \mathbf{R}_j^{+-} \mathbf{E}_j^{--} \bar{\mathbf{S}}^{ext,-} \\ & + \mathbf{R}_j^{+-} \mathbf{E}_j^{-+} \bar{\mathbf{S}}^{ext,+} \\ & + \mathbf{T}_j^{++} \bar{\mathbf{j}}^{+L} + \mathbf{E}_j^{+-} \bar{\mathbf{S}}^{ext,-} + \mathbf{E}_j^{++} \bar{\mathbf{S}}^{ext,+})) + \mathbf{E}_j^{+-} \bar{\mathbf{S}}^{ext,-} + \mathbf{E}_j^{++} \bar{\mathbf{S}}^{ext,+} \end{aligned} \quad (39)$$

Collecting the terms that operate on the current coming in both sides a new  $\mathbf{m}^{out,in}$  matrix is created for the merged cell which can be separated into new  $\mathbf{T}$  and  $\mathbf{R}$  sub-matrices. Using the example from figures 6 through 11, using the number of merges  $n = 3$  and going through the merges as  $i = n$  to 1 using steps of -1 the new sub-matrices are:

$$\mathbf{T}_{(i-1)j}^{--} = \mathbf{T}_{(i)j}^{--} (\mathbf{I} - \mathbf{R}_{(i)j}^{-+} \mathbf{R}_{(i)j}^{+-})^{-1} \mathbf{T}_{(i)j}^{--}, \quad (40)$$

$$\mathbf{R}_{(i-1)j}^{-+} = \mathbf{T}_{(i)j}^{--} (\mathbf{I} - \mathbf{R}_{(i)j}^{-+} \mathbf{R}_{(i)j}^{+-})^{-1} \mathbf{R}_{(i)j}^{-+} \mathbf{T}_{(i)j}^{++} + \mathbf{R}_{(i)j}^{-+}, \quad (41)$$

$$\mathbf{R}_{(i-1)j}^{+-} = \mathbf{R}_{(i)j}^{+-} + \mathbf{T}_{(i)j}^{++} (\mathbf{I} - \mathbf{R}_{(i)j}^{-+} \mathbf{R}_{(i)j}^{+-})^{-1} \mathbf{R}_{(i)j}^{+-} \mathbf{T}_{(i)j}^{--}, \quad (42)$$

$$\mathbf{T}_{(i-1)j}^{++} = \mathbf{T}_{(i)j}^{++} (\mathbf{I} - \mathbf{R}_{(i)j}^{+-} \mathbf{R}_{(i)j}^{-+})^{-1} \mathbf{T}_{(i)j}^{++}. \quad (43)$$

Following this example, the original  $\mathbf{m}^{out,in}$  matrix, at level  $n = 3$  (sub-cell thickness  $= \frac{1}{2^3} = \frac{1}{8}$ ), was

$$\mathbf{m}^{out,in} = \begin{pmatrix} \mathbf{T}_{(3)j}^{--} & \mathbf{R}_{(3)j}^{-+} \\ \mathbf{R}_{(3)j}^{+-} & \mathbf{T}_{(3)j}^{++} \end{pmatrix} \quad (44)$$

After 3 merges, at each level replacing the old sub-matrices with the new merged-cell  $\mathbf{m}^{out,in}$  matrix is:

$$\mathbf{m}^{out,in} = \begin{pmatrix} \mathbf{T}_{(0)j}^{--} & \mathbf{R}_{(0)j}^{-+} \\ \mathbf{R}_{(0)j}^{+-} & \mathbf{T}_{(0)j}^{++} \end{pmatrix}, \quad (45)$$

with a new cell thickness of  $\frac{1}{2^0} = 1$ .

A similar exercise can be done for the terms that operate on the external emission source going in each direction of the cell. A new  $\mathbf{m}^{out,ext}$  is created for the combined cell that can also be separated into new  $\mathbf{E}$  sub-matrices.

$$\begin{aligned} \mathbf{E}_{(i-1)j}^{--} &= \mathbf{T}_{(i)j}^{--}(\mathbf{I} - \mathbf{R}_{(i)j}^{-+}\mathbf{R}_{(i)j}^{+-})^{-1}\mathbf{R}_{(i)j}^{-+}\mathbf{E}_{(i)j}^{+-} + \\ &\quad \mathbf{T}_{(i)j}^{--}(\mathbf{I} - \mathbf{R}_{(i)j}^{-+}\mathbf{R}_{(i)j}^{+-})^{-1}\mathbf{E}_{(i)j}^{--} + \mathbf{E}_{(i)j}^{--} \end{aligned} \quad (46)$$

$$\begin{aligned} \mathbf{E}_{(i-1)j}^{-+} &= \mathbf{T}_{(i)j}^{--}(\mathbf{I} - \mathbf{R}_{(i)j}^{-+}\mathbf{R}_{(i)j}^{+-})^{-1}\mathbf{R}_{(i)j}^{-+}\mathbf{E}_{(i)j}^{++} + \\ &\quad \mathbf{T}_{(i)j}^{--}(\mathbf{I} - \mathbf{R}_{(i)j}^{-+}\mathbf{R}_{(i)j}^{+-})^{-1}\mathbf{E}_{(i)j}^{-+} + \mathbf{E}_{(i)j}^{-+} \end{aligned} \quad (47)$$

$$\begin{aligned} \mathbf{E}_{(i-1)j}^{+-} &= \mathbf{T}_{(i)j}^{++}(\mathbf{I} - \mathbf{R}_{(i)j}^{+-}\mathbf{R}_{(i)j}^{-+})^{-1}\mathbf{R}_{(i)j}^{+-}\mathbf{E}_{(i)j}^{--} + \\ &\quad \mathbf{T}_{(i)j}^{++}(\mathbf{I} - \mathbf{R}_{(i)j}^{+-}\mathbf{R}_{(i)j}^{-+})^{-1}\mathbf{E}_{(i)j}^{+-} + \mathbf{E}_{(i)j}^{+-} \end{aligned} \quad (48)$$

$$\begin{aligned} \mathbf{E}_{(i-1)j}^{++} &= \mathbf{T}_{(i)j}^{++}(\mathbf{I} - \mathbf{R}_{(i)j}^{+-}\mathbf{R}_{(i)j}^{-+})^{-1}\mathbf{R}_{(i)j}^{+-}\mathbf{E}_{(i)j}^{-+} + \\ &\quad \mathbf{T}_{(i)j}^{++}(\mathbf{I} - \mathbf{R}_{(i)j}^{+-}\mathbf{R}_{(i)j}^{-+})^{-1}\mathbf{E}_{(i)j}^{++} + \mathbf{E}_{(i)j}^{++} \end{aligned} \quad (49)$$

Similar to (45) the merged-cell  $\mathbf{m}^{out,ext}$  is:

$$\mathbf{m}^{out,ext} = \begin{pmatrix} \mathbf{E}_{(0)j}^{--} & \mathbf{E}_{(0)j}^{-+} \\ \mathbf{E}_{(0)j}^{+-} & \mathbf{E}_{(0)j}^{++} \end{pmatrix} \quad (50)$$

By merging the sub-matrices in this way and then reassembling the  $\mathbf{m}$  matrices after each merge, this algorithm can be repeated  $n$  times, giving a final set of  $m$  matrices that can now act on the current coming into the cell and the external emission source in the cell to produce a current out of the cell in each direction. These directions can then be summed over the ordinate weights to give a partial current out of the cell in each direction that has the accuracy of  $2^n$  cells each of which is  $2^{-n}$  thick. A simplified version can be seen in Algorithm 2. As can be seen in the above matrices, a matrix inversion is required during each merging of cells. This is a possible point of bad conditioning of the matrices. By numerically taking inverses of matrices, loss of good digits can occur. For this method I used a Gaussian Elimination with Partial Pivot routine [16] that ensured a maximum conditioning of the matrices during each merge.

### III. TESTING

In order to test this new approach to DI, it was necessary to verify that it accurately solves for the partial currents out of the cell and the average scalar flux in the cell. This is done by comparing the solutions from this algorithm to solutions from a benchmark solution achieved from an SI code. Once the code is shown to be capable of achieving the same solutions as SI then the code can be tested against that same benchmark to demonstrate its ability to reach the same solution with fewer computations than the SI code.

#### *III.A. Verification Testing*

To verify the accuracy of my code, I used an SI code [18] that uses various input and material parameters to solve for the currents out of each cell and the average scalar flux in the cell. The parameters for the SI code include: Ordinate set, illumination on each side of the cell (current in), emission source in the cell, total cross section ( $\sigma_t$ ), and scattering ratio ( $c = \sigma_t / \sigma_s$ ). Each of these parameters was adjusted in various combinations. The SI code was run until it reached a limit where it ceased to change with a tolerance of  $10^{-16}$ . This allowed me to compare the answer between my DI method and SI to 16 digits. The SI code is capable of using the Step, SC, DD and EC spatial quadratures. Because my approach is only concerned with spatial quadratures that are positive and linear, the verification portion of the testing only compares the two methods that meet these criteria, Step and SC. Due to the fact that Step and SC are only first-order accurate methods, the key to attaining accuracy comparable to the higher-order methods is to, in the case of SI, create a finer mesh with cells that are optically thinner, and then perform the calculations through the thinner celled problem. In section II of this document I presented how this was to be achieved with my method, by subdividing the cell, and then repeatedly merging



sets of two sub-cells at a time until the original cell is solved. Various cell divisions were tested to verify that there was no loss of precision in my method.

Step 1 in the verification process is to ensure that the arithmetic of my method is valid. I did this by setting up a series of conditions in my method that would let me verify that the individual entries in the  $\mathbf{m}$  matrices were correct. To do this I used the following problem definitions:

- Vacuum boundaries on both sides of the cell
- Number of divisions (for my method) = 4
- Cell mesh refinement (for SI code) = 256
- Angular quadrature =  $S_4$
- $\sigma = .80$
- $c = .65$
- $\Delta x = 20$  (mfp =  $\sigma \Delta x = 16$ )

Using the matrix form of (21) and setting all but one entry in  $\vec{j}^{in}$  to 0, and all of  $\vec{S}^{ext}$  to 0,  $\vec{j}^{out}$  should equal the first column in  $\mathbf{m}^{out,in}$ .

$$\vec{j}^{out} = \begin{pmatrix} m^{out,in}_{1,1} \\ m^{out,in}_{2,1} \\ m^{out,in}_{3,1} \\ m^{out,in}_{4,1} \end{pmatrix} = \begin{pmatrix} m^{out,in}_{1,1} & m^{out,in}_{1,2} & m^{out,in}_{1,3} & m^{out,in}_{1,4} \\ m^{out,in}_{2,1} & m^{out,in}_{2,2} & m^{out,in}_{2,3} & m^{out,in}_{2,4} \\ m^{out,in}_{3,1} & m^{out,in}_{3,2} & m^{out,in}_{3,3} & m^{out,in}_{3,4} \\ m^{out,in}_{4,1} & m^{out,in}_{4,2} & m^{out,in}_{4,3} & m^{out,in}_{4,4} \end{pmatrix} \begin{pmatrix} j^{in}_{\mu 1} \\ j^{in}_{\mu 2} \\ j^{in}_{\mu 3} \\ j^{in}_{\mu 4} \end{pmatrix} + m^{out,ext} \cdot \vec{0} \quad (51)$$

where  $j^{in}_{\mu 1} = 1$ , and  $j^{in}_{\mu 2} = j^{in}_{\mu 3} = j^{in}_{\mu 4} = 0$ . This process was then repeated setting each consecutive entry of  $\vec{j}^{in}$  to 1 and the rest to zero, and then doing the same for the  $\vec{S}^{ext}$  vector. I used the same input variables and conditions for the SI code and compared the results (for Step and SC) for each column of the  $\mathbf{m}$  matrices. Using this scheme the Symmetric Relative Difference (SRD) between SI and my method was on the order of  $10^{-13}$ . Based on these results, I conclude that my method is calculating the within-cell transport correctly.

### III.B. Performance Testing

In order to test the performance of the merging approach to DI, the EC method of SI was used as the benchmark. Even though it is not a linear method, it has been shown [15] that it has a high order of accuracy (4) and converges faster than any of the other methods contained in the SI code. It also has the benefit of being an unconditionally positive quadrature.

In order to use EC as a benchmark, I ran the SI code multiple times using an  $S_8$  angular quadrature, each run increasing the sub-cell mesh until the average scalar flux (for test problems 1, 2, and 3) and the partial current (for test problem 4) stopped changing at  $10^{-6}$ . For EC this took a mesh refinement of  $2^5$  (32) sub-cells for a scattering ratio of  $c=.25$  and  $2^6$  (64) sub-cells for  $c=.5$  and  $c=.75$ . Once the benchmark was set, I repeated the process for each of the other three spatial quadratures in the SI code, ST, SC, and DD, until the difference between it and the benchmark, for average scalar flux (test problems 1 and 2) and the partial current (test problem 3) was less than  $10^{-6}$ . I repeated this process using my code and compared the results of the SI code and my code (using Step and SC) in order to verify that my code was obtaining the same answers. The results of this series of tests show that for several different combinations of input and material properties that my method was consistent with SI methods (Step and SC) with an SRD  $< 10^{-13}$  for problems that had low scattering ratios and were not optically thick.

However, as the cell was divided many times, with the original cell thickness becoming optically thick and the scattering ratio increasing, as subsequent tests will reveal, the answers began to lose accuracy. Using Step the two methods began to diverge after 7 divisions (128 mesh refinement) with an SRD  $< 10^{-12}$ . At 10 cell divisions (1024 mesh refinement) the two methods had an SRD  $< 10^{-11}$ . At 12 cell divisions (4096 mesh refinement) the two methods had an SRD  $< 10^{-10}$ . Even after 20 divisions (1048576 mesh refinement) only had an SRD  $< 10^{-7}$ . This loss of digits is most likely due to calculating the multiple matrix inverses that are required during each merge of the  $\mathbf{m}$  matrices. Even though the matrices are

very well conditioned (matrix condition number  $\approx 1$  for low to mid-range scattering media), the loss of precision after 7 divisions results in a negligible loss of digits. This is further investigated in section III.C, *Matrix Conditioning*.

### III.B.1 Test Problem 1: Scattering Ratio ( $c$ ) = .25

This test problem is characteristic of a high absorbing material with an emission source within the material. The parameters for this test were:

- Vacuum boundaries on both sides of the cell
- Angular quadrature =  $S_8$
- $\sigma = .75$
- $c = .25$
- $\Delta x = 2$  (mfp = 1.5)
- $\vec{S}^{ext} = 2$
- $\vec{J}_L^{in} = \vec{J}_R^{in} = 2$

The results of the test are contained in Table 3 and a visual graphic display shown in Figure 13.

Table 2: Test Problem 1 Results

Spatial Quadrature	Mesh Refinement/No of Merges (No. of sub-cells)	Number of Iterations (SI)/ Number of Merges (DI)	Time to Reach Limit [s]
SI: EC	32	23	0.078
SI: DD	64	25	0.063
SI: ST	131072	25	6.45
SI: SC	512	26	0.125
DI: ST	17	17	0
DI: SC	9	9	0.016

As shown in these results, for this type of material DD is a good performer. However, looking only at average scalar flux can be deceiving in that the negative individual vector components of the flux can be negative, which as stated before are non-physical and hence meaningless. As can be seen in the table Step using SI required a mesh refinement of 131,072 sub-cells in order to come to within  $10^{-6}$

of the benchmark. Step using DI, however, only required 17 merges to achieve the same results. This results in much less computational time.

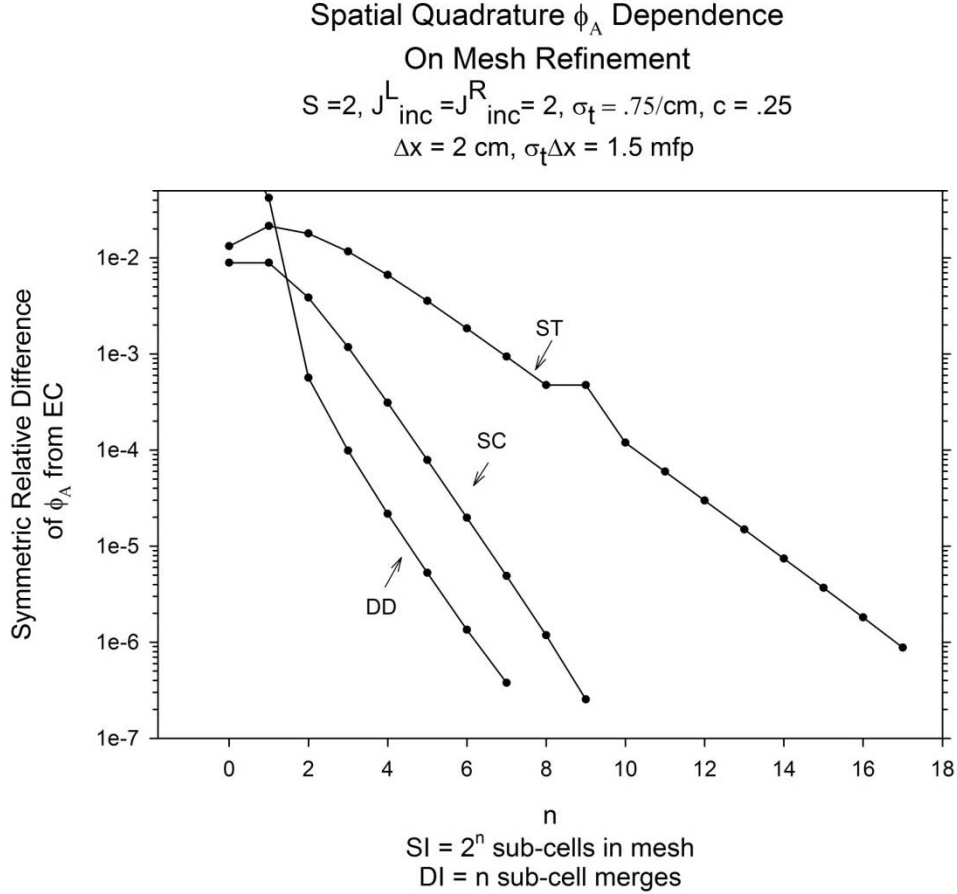


Figure 13: Test Problem 1:  $c = .25$

### III.B.2 Test Problem 2: Scattering Ratio ( $c$ ) = .75

Using the same source and incident currents as Test Problem 1, this test increased the scattering ratio to 0.75, characteristic of a high scatter medium.

The set of parameters for this test are:

- Vacuum boundaries on both sides of the cell
- Angular quadrature =  $S_8$

- $\sigma = .75$
- $c = .75$
- $\Delta x = 2$  (mfp = 1.5)
- $\vec{S}^{ext} = 2$
- $\vec{j}_L^{in} = \vec{j}_R^{in} = 2$

This case is similar to Test Problem 1, but the average flux in the cell becomes more difficult for SI to achieve the correct answer, requiring a more refined cell and more computational time.

**Table 3: Test Problem 2 Results**

Spatial Quadrature	Mesh Refinement/No of Merges (No. of sub-cells)	Number of Iterations (SI)/ Number of Merges (DI)	Time to Reach Limit [s]
SI: EC	64	61	0.156
SI: DD	512	64	0.125
SI: ST	262144	65	20.48
SI: SC	512	67	0.219
DI: ST	18	18	0
DI: SC	9	9	0

As shown in Table 4, DD continues to approach the same limit as EC quickly but requires twice the cell refinement in order to do so. SC in this case requires no more refinement to approach the same limit as EC as before in test 1, but does require more computational time because of the increase scattering ratio. In both cases of the DI routines, even though the number of merges increased, the effective computational cost did not. This shows the strength of this new approach. Figure 14 shows a similar pattern for this test as for test 1.

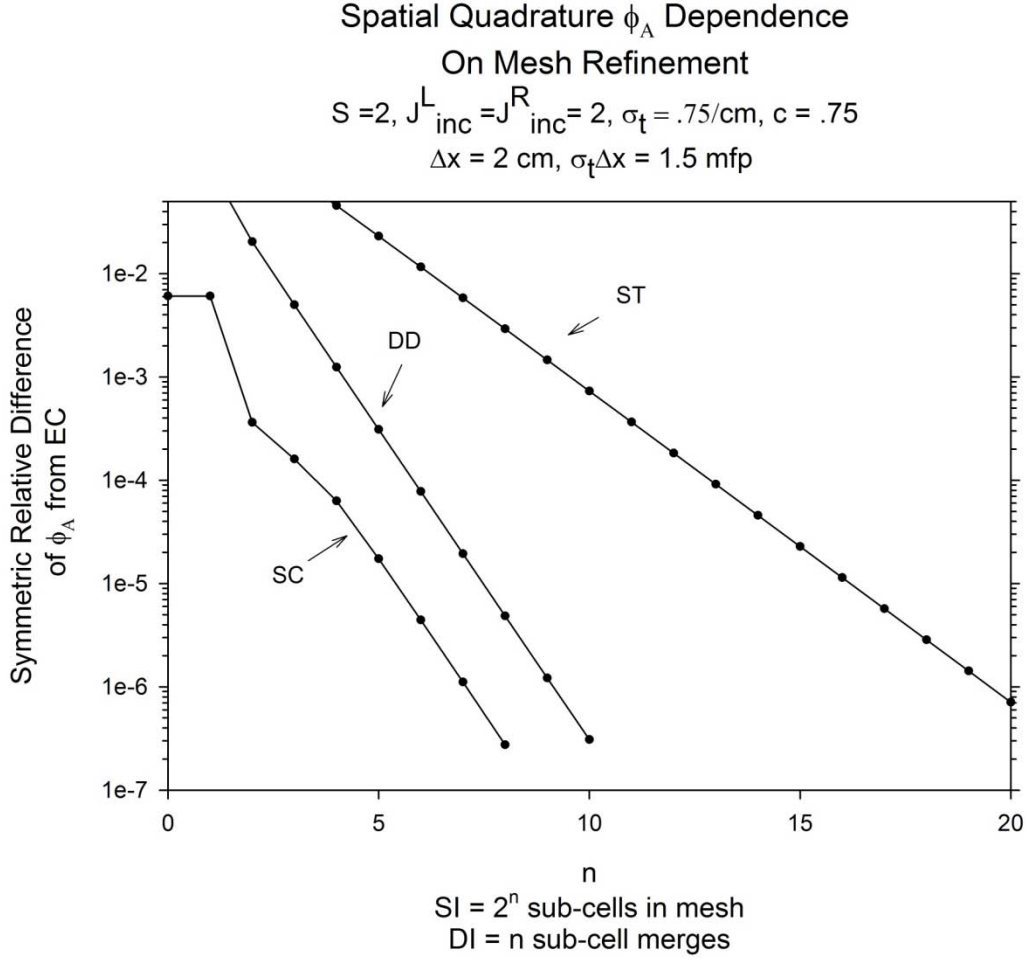


Figure 14: Test Problem 2:  $c = .75$

### III.B.3 Test Problem 3: No Source, Current in on One Side

In this test, the parameters of the problem were changed to be a medium with no external source, incident current on the left side of the cell only, and the width of the cell beginning at 3 mfp instead of 1.5. The results of this test are summarized in Table 5. The set of parameters for this test are:

- Vacuum boundaries on both sides of the cell
- Angular quadrature =  $S_8$
- $\sigma = .75$
- $c = .75$

- $\Delta x = 4$  (mfp = 3)
- $\vec{S}^{ext} = 0$
- $\vec{J}_L^{in} = 2$
- $\vec{J}_R^{in} = 0$

Table 4: Test Problem 3 Results

Spatial Quadrature	Mesh Refinement/No of Merges (No. of sub-cells)	Number of Iterations (SI)/Number of Merges (DI)	Time to Reach Limit [s]
SI: EC	64	88	0.359
SI: DD	1024	93	0.594
SI: ST	262144	89	33.4
SI: SC	512	89	0.594
DI: ST	18	18	0
DI: SC	9	9	0

The results of this test show the weakness of DD in that when the cell is optically thick ( $>2$  mfp) the partial currents on the far side of the cell are negative until the mesh refinement is high enough. This negative current is shown in Figure 15.

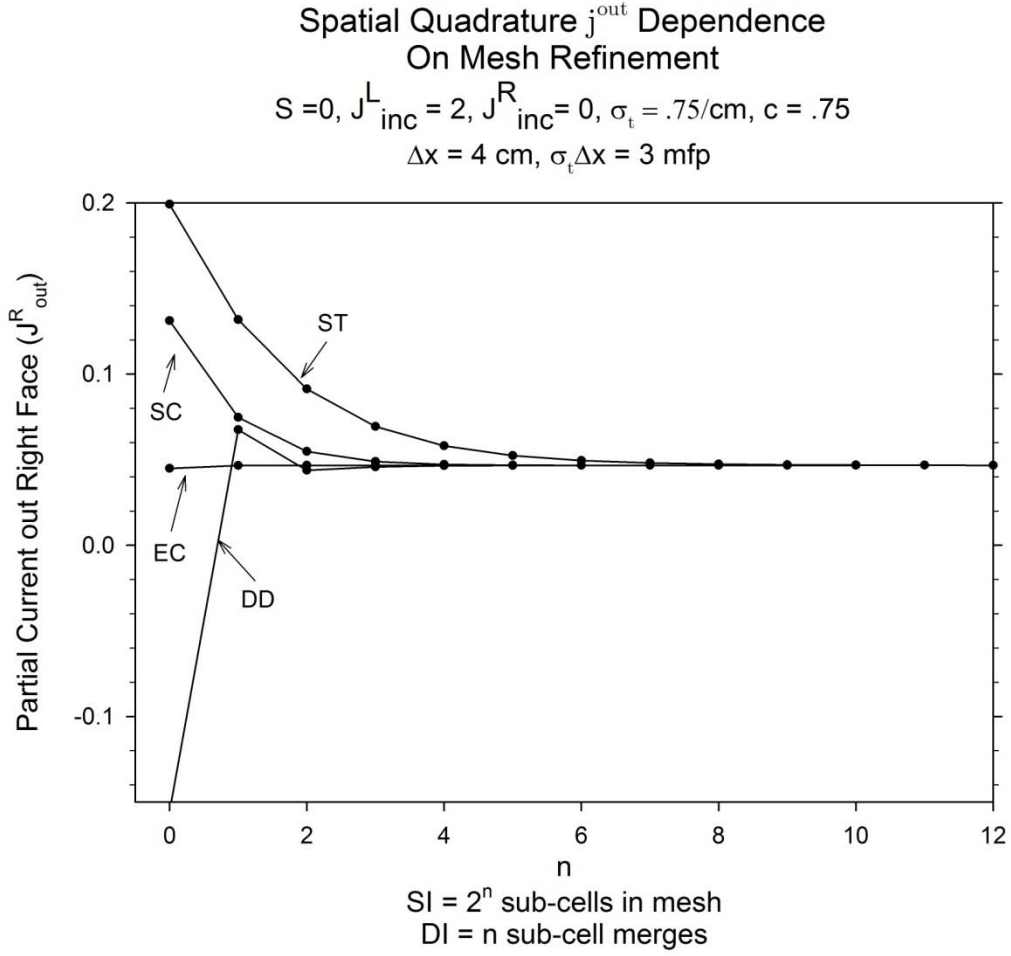


Figure 15: Test Problem 3: No Source, One Current

#### III.B.4 Test Problem 4: Approaching Diffusion

The final test that was conducted is one that tests the limits of discrete ordinates methods, that of a diffusion problem where  $c = 1$  and the cell is many mean free paths thick. In order to do this, I set the problem parameters to:

- Vacuum boundaries on both sides of the cell
- Angular quadrature =  $S_8$
- $\sigma = .75$
- $c = .99$
- $\Delta x = 2$  (mfp = 1.5)
- $\vec{S}^{\text{ext}} = 0$



- $\vec{j}_L^{in} = \vec{j}_R^{in} = 0$

The benchmark SI code used was not able to reach a limit for  $c = 1$ . Therefore, for this test, the scattering ratio only approaches 1, hence it approaches diffusion. Even at  $c = .99$  only the SI quadrature of EC was able to reach a limit in a timely manner requiring over 1100 sweeps to stop changing at  $10^{-6}$ . This brings to question the validity of the results, but serves as a decent comparison between the computational speeds of this method and those of SI. The results of this test are shown in Figure 16.

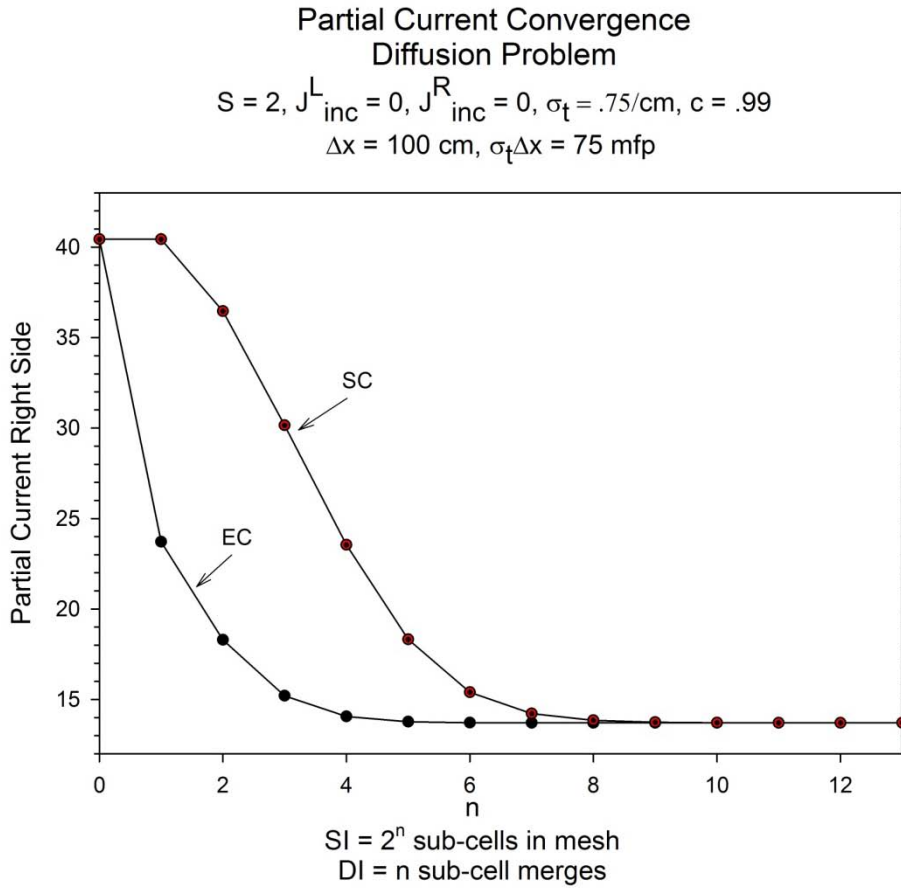


Figure 16: Test Problem 4: Approaching Diffusion

As can be seen from the figure, DI:SC reached the same limit for partial current as SI:EC. As stated above, EC required over 1100 sweeps to reach this limit, and this had to be done through  $2^{10}$  sub-cells. This required a real time solution of approximately 1 minute. DI required 13 merges to reach the same solution, requiring computational time of 0.0156 seconds.

### *III.C. Matrix Conditioning*

As stated earlier, the number of matrix inversions is a possible point of loss of precision in my method. The following tests show how the condition number of the matrix varies with different problem parameters, including the number of merges required to achieve the accuracy of high-order spatial quadratures. In each of these tests I used the infinity-norms of the matrices in order to calculate the condition numbers.

#### *III.C.1 Condition Number vs. Cell Thickness (Optical) ( $c = .1$ )*

The first parameter to investigate is cell thickness in terms of the optical thickness of the medium. The parameters for this set of tests are the following:

- Vacuum boundaries on both sides of the cell
- Angular quadrature =  $S_8$
- $\sigma = 1$
- $c = .1$
- Original cell  $\Delta x$  (varies) = 1 to 1024 mfp
- $\vec{S}^{ext} = 5$
- $\vec{J}_L^{in} = 2$
- $\vec{J}_R^{in} = 3$
- Number of merges = 20

Based on the results of this test the condition number went no higher than 1.0017. This demonstrates that a problem with a low scattering ratio the cells can be very optically thick without increasing the condition number with 20 merges. My method is well conditioned for this set of parameters. For this problem, using a high absorbing medium, my method can take a cell that has an

optical thickness of 1024 mean free paths, and using a first-order, linear, positive spatial quadrature, achieve the same accuracy as if the cell was 1/1000 the thickness of a mean free path.

### *III.C.2 Condition Number vs. Cell Thickness (Optical) ( $c = .9$ )*

In this test I use the same parameters as those in the last section except for the scattering ratio, which I now set at  $c = .9$ . This is a high scattering medium. The results for this test are shown in Table 6. In this table the first column is the merge number. For example, merge #1 is the first merge of two of the most optically thin sub-cells. Merge #20 is the last merge of the two half sub-cells to make result in the original cell. This is true for both of the next two tables.

The results for this test are comparable to the previous test, showing that within the range of scattering ratios, from  $c = .1$  to  $c = .9$ , the thickness of the cell does not have a significant effect on the conditioning of the matrices.

Table 5: Condition Number vs. Cell Thickness ( $c = 0.9$ )

	Cell Thickness (Optical) $c = .9$										
Merge #	1	2	4	8	16	32	64	128	256	512	1024
1	1.0000	1.0000	1.0000	1.0000	1.0000	1.0000	1.0000	1.0000	1.0000	1.0000	1.0000
2	1.0000	1.0000	1.0000	1.0000	1.0000	1.0000	1.0000	1.0000	1.0000	1.0000	1.0000
3	1.0000	1.0000	1.0000	1.0000	1.0000	1.0000	1.0000	1.0000	1.0000	1.0000	1.0001
4	1.0000	1.0000	1.0000	1.0000	1.0000	1.0000	1.0000	1.0000	1.0000	1.0001	1.0002
5	1.0000	1.0000	1.0000	1.0000	1.0000	1.0000	1.0000	1.0000	1.0001	1.0002	1.0008
6	1.0000	1.0000	1.0000	1.0000	1.0000	1.0000	1.0000	1.0001	1.0002	1.0008	1.0029
7	1.0000	1.0000	1.0000	1.0000	1.0000	1.0000	1.0001	1.0002	1.0008	1.0029	1.0105
8	1.0000	1.0000	1.0000	1.0000	1.0000	1.0001	1.0002	1.0008	1.0029	1.0105	1.0342
9	1.0000	1.0000	1.0000	1.0000	1.0001	1.0002	1.0008	1.0029	1.0105	1.0342	1.0980
10	1.0000	1.0000	1.0000	1.0001	1.0002	1.0008	1.0029	1.0105	1.0343	1.0982	1.2417
11	1.0000	1.0000	1.0001	1.0002	1.0008	1.0029	1.0105	1.0343	1.0982	1.2419	1.5086
12	1.0000	1.0001	1.0002	1.0008	1.0029	1.0105	1.0343	1.0982	1.2420	1.5089	1.8572
13	1.0001	1.0002	1.0008	1.0029	1.0105	1.0343	1.0983	1.2421	1.5091	1.8577	2.0659
14	1.0002	1.0008	1.0029	1.0105	1.0343	1.0983	1.2421	1.5091	1.8579	2.0663	2.0974
15	1.0008	1.0029	1.0105	1.0343	1.0983	1.2421	1.5092	1.8580	2.0665	2.0978	2.0979
16	1.0029	1.0105	1.0343	1.0983	1.2421	1.5092	1.8580	2.0667	2.0980	2.0983	2.0979
17	1.0105	1.0343	1.0983	1.2421	1.5092	1.8581	2.0667	2.0981	2.0985	2.0983	2.0979
18	1.0343	1.0983	1.2421	1.5092	1.8581	2.0667	2.0982	2.0986	2.0985	2.0983	2.0979
19	1.0983	1.2421	1.5092	1.8581	2.0668	2.0982	2.0987	2.0986	2.0985	2.0983	2.0979
20	1.2421	1.5092	1.8581	2.0668	2.0982	2.0987	2.0987	2.0986	2.0985	2.0983	2.0979

### III.C.3 Condition Number vs. Cell Thickness (Optical) ( $c = 1$ )

This test focuses on a pure scattering medium, a problem that is not possible for SI codes to solve. Using all the same parameters, changing the scattering ratio to  $c = 1$ , I ran the same problem, using cell thicknesses from 1 mean free path to 1024 mean free paths. The results are shown in Table 7.

**Table 6: Condition Number vs. Cell Thickness ( $c = 1$ )**

	Cell Thickness (Optical) $c = 1$										
Merge #	1	2	4	8	16	32	64	128	256	512	1024
1	1.0000	1.0000	1.0000	1.0000	1.0000	1.0000	1.0000	1.0000	1.0000	1.0000	1.0000
2	1.0000	1.0000	1.0000	1.0000	1.0000	1.0000	1.0000	1.0000	1.0000	1.0000	1.0000
3	1.0000	1.0000	1.0000	1.0000	1.0000	1.0000	1.0000	1.0000	1.0000	1.0000	1.0001
4	1.0000	1.0000	1.0000	1.0000	1.0000	1.0000	1.0000	1.0000	1.0000	1.0001	1.0002
5	1.0000	1.0000	1.0000	1.0000	1.0000	1.0000	1.0000	1.0000	1.0001	1.0002	1.0010
6	1.0000	1.0000	1.0000	1.0000	1.0000	1.0000	1.0000	1.0001	1.0002	1.0010	1.0037
7	1.0000	1.0000	1.0000	1.0000	1.0000	1.0000	1.0001	1.0002	1.0010	1.0037	1.0132
8	1.0000	1.0000	1.0000	1.0000	1.0000	1.0001	1.0002	1.0010	1.0037	1.0132	1.0440
9	1.0000	1.0000	1.0000	1.0000	1.0001	1.0002	1.0010	1.0037	1.0132	1.0440	1.1320
10	1.0000	1.0000	1.0000	1.0001	1.0002	1.0010	1.0037	1.0132	1.0441	1.1321	1.3570
11	1.0000	1.0000	1.0001	1.0002	1.0010	1.0037	1.0132	1.0441	1.1322	1.3573	1.9107
12	1.0000	1.0001	1.0003	1.0010	1.0037	1.0132	1.0441	1.1322	1.3574	1.9113	3.2696
13	1.0001	1.0003	1.0010	1.0037	1.0132	1.0441	1.1322	1.3575	1.9116	3.2707	6.4441
14	1.0003	1.0010	1.0037	1.0132	1.0441	1.1322	1.3575	1.9117	3.2713	6.4466	13.3319
15	1.0010	1.0037	1.0132	1.0441	1.1322	1.3575	1.9118	3.2716	6.4479	13.3372	27.5573
16	1.0037	1.0132	1.0441	1.1322	1.3575	1.9118	3.2718	6.4485	13.3398	27.5678	56.3169
17	1.0132	1.0441	1.1322	1.3576	1.9118	3.2718	6.4488	13.3411	27.5731	56.3380	114.0213
18	1.0441	1.1322	1.3576	1.9118	3.2719	6.4490	13.3418	27.5758	56.3486	114.0636	229.5322
19	1.1322	1.3576	1.9118	3.2719	6.4491	13.3421	27.5771	56.3539	114.0848	229.6167	460.6076
20	1.3576	1.9118	3.2719	6.4491	13.3423	27.5778	56.3566	114.0954	229.6590	460.7765	922.7858

The results of this test show that for a scattering medium the matrices become ill-conditioned as the cell thickness increases and the number of merges increases. I shaded a rough diagonal in Table 7, showing a possible acceptable limit of my method with these parameters where the matrices are well-conditioned. This shows that for a given cell thickness a certain number of merges can be performed before an unacceptable loss of good digits occurs. For example, if I were to begin with a cell of optical thickness = 256 mean free paths, I could expect to be able to merge sub-cells that are  $2^{-14}$  -  $2^{-16}$  the thickness of the original cell before the results are suspect.

### *III.C.4 Condition Number Dependence on Angular Quadrature*

The dependence of the matrix condition number on the angular quadrature used is a straightforward exercise. As the number of ordinates increases, the size of the matrix increases. For example,  $S_4$  creates a 4 x 4 **m** matrix.  $S_8$  creates a 8 x 8 **m** matrix. Because the **m** matrices are almost diagonal, with values near 1 on the diagonal and very small numbers off the diagonal, the condition number does not increase and is therefore not dependant on the number of ordinates, for low to mid-range scattering media. However, as seen in Table 7, when I tested a pure scattering medium the condition number increased with the number of merges. After testing  $S_4 - S_{32}$  I found that the condition number is not dependant on the number of ordinates, but rather on the scattering ratio of the medium. The following is a list of approximate condition numbers for the low-scattering media through all 20 merges:

<u>Angular Quadrature</u>	<u>Approximate Condition Number</u>
$S_4$	1
$S_8$	1
$S_{16}$	1
$S_{32}$	1

## IV. SUMMARY

### *IV.A. Achievement of Objectives*

*Increased Accuracy:* As has been shown, in order to increase accuracy for the linear, positive spatial quadratures the thickness of the cell has to be decreased. In the past, for SI models, this has been done by refining the spatial mesh into many smaller cells. This increases the computational time required to sweep through the mesh. For Slab geometry the increase can be very substantial. Extending that to 2 and 3-D geometries can become devastating.

This new algorithm for DI shows that it can achieve the same accuracy using Step and SC spatial quadratures as that of a higher order method. The bonus to this fact is that it required orders of magnitude fewer computations to achieve the same result.

*Numerical Stability:* Going into this project, knowing that the algorithm required matrix inversions for each merge process, I knew that stability issues might arise. Matrix inversions, if not done carefully, can result in the loss of digits. For the range of optical thicknesses and angular quadrature sets with isotropic scattering tested here, the matrices were remarkably well-conditioned resulting in very little loss of good digits in the number of merges performed to attain the required accuracy, except where the medium was very optically thick and diffusive.

*Integration into DI Code:* The method that I developed has not been integrated with the existing 1-D DI code. The DI code computes the  $\mathbf{m}^{out,in}$  matrix before solving the global partial current problem which my method could be used in place of the current method. It does not, however, treat the coefficients of the external emission source as matrix in the same way that I did. Generating both matrices was a key part of the merging process. This may require some modification of the DI code in order for it to use my method.

#### *IV.B. Future Work*

As discussed this method requires integration into the 1-D DI code. Extending this method to 2 and 3-D geometries will require much more work, but if achievable, can produce a new method that will out-perform SI codes that are currently being used. Conditioning of the matrices can be improved by applying different matrix inversion schemes. This will allow more cell merges, if necessary, allowing the starting cell thickness to be more mean free paths thick.

#### *IV.C. Observations and Conclusions*

In conclusion, this new algorithm that can be used by the DI discrete ordinates method does show promise in its ability to increase the accuracy of spatial quadratures that are linear and unconditionally positive. This will overcome the some of the issues that discrete ordinates methods have had, namely non-physical negative results that come from spatial quadratures that are not unconditionally positive and solutions that do not approach an appropriate diffusion limit that happens with non-linear methods. The results showed very good numerical stability and very short computational times.



## APPENDIX A

### K MATRICES FOR STEP

The K matrices are defined by the spatial quadrature and the balance equation.

$$\text{Let } \varepsilon_n = \frac{\sigma \Delta x}{|\mu_n|}$$

$$K_{n,n}^{out,in} = \frac{1}{1 + \varepsilon_n} \quad (52)$$

$$K_{n,n}^{out,s} = \frac{\Delta x}{1 + \varepsilon_n} \quad (53)$$

$$K_{n,n}^{\psi,in} = \frac{1/|\mu_n|}{1 + \varepsilon_n} \quad (54)$$

$$K_{n,n}^{\psi,s} = \frac{\Delta x / |\mu_n|}{1 + \varepsilon_n} \quad (55)$$

As is explained by Mathews [14], for an isotropic source, like the source in the examples that I used to test my method the following applies:

$$K_{n,n}^{out,ext} = K_{n,n}^{out,s} = \frac{\Delta x}{1 + \varepsilon_n} \quad (56)$$

and

$$K_{n,n}^{\psi,ext} = K_{n,n}^{\psi,s} = \frac{\Delta x / |\mu_n|}{1 + \varepsilon_n} \quad (57)$$

All of these matrices are diagonal and symmetric.

## APPENDIX B

### K MATRICES FOR STEP CHARACTERISTIC

The K matrices are defined by the spatial quadrature and the balance equation.

$$K_{n,n}^{out,in} = e^{-\varepsilon_n} \quad (58)$$

where

$$\varepsilon_n = \sigma \Delta x / \mu_n \quad (59)$$

$$K_{n,n}^{out,s} = \frac{(1 - e^{-\varepsilon_n}) \mu_n}{\sigma} \quad (60)$$

$$K_{n,n}^{\psi,in} = \frac{\mathcal{M}_0(\varepsilon_n)}{|\mu_n|} \quad (61)$$

where the zeroth exponential moment function is defined as:

$$\mathcal{M}_0(\varepsilon) = \frac{(1 - e^{-\varepsilon})}{\varepsilon} \quad (62)$$

$$K_{n,n}^{\psi,s} = \frac{\Delta x}{|\mu_n|} \mathcal{M}_1(\varepsilon_n) \quad (63)$$

where the first exponential moment function is defined as:

$$\mathcal{M}_1(\varepsilon_n) = \frac{(1 - \mathcal{M}_0(\varepsilon_n))}{\varepsilon_n} \quad (64)$$

Because the problem is isotropic SC follows Step in that:

$$K_{n,n}^{out,ext} = K_{n,n}^{out,s} = \frac{(1 - e^{-\varepsilon_n}) \mu_n}{\sigma \Delta x} \Delta x = \Delta x \mathcal{M}_0(\varepsilon_n) \quad (65)$$

and:

$$K_{n,n}^{\psi,ext} = K_{n,n}^{\psi,s} = \frac{\Delta x}{|\mu_n|} \mathcal{M}_1(\varepsilon_n) \quad (66)$$

## APPENDIX C

### M MATRICES FOR FLUX

The algorithms for computing and merging the m coefficient matrices that act on flux are similar to those that were presented in Section II.C.1 of the thesis. However, because flux coming into the cell creates flux and current, the matrices for flux are slightly more complicated.

Beginning with equations (25) and (26) I split the cell into two identical sub-cells of  $\frac{1}{2}$  dx thicknesses and have these two equations for each cell with currents at the center:

$$\psi_L^- = \mathbf{T}_\psi^{--} \vec{\mathbf{j}}^{-C} + \mathbf{R}_\psi^{-+} \vec{\mathbf{j}}^{+L} + \mathbf{E}_\psi^{--} \vec{\mathbf{S}}^{ext,-} + \mathbf{E}_\psi^{-+} \vec{\mathbf{S}}^{ext,+} \quad (67)$$

$$\psi_L^+ = \mathbf{R}_\psi^{+-} \vec{\mathbf{j}}^{-C} + \mathbf{T}_\psi^{++} \vec{\mathbf{j}}^{+L} + \mathbf{E}_\psi^{+-} \vec{\mathbf{S}}^{ext,-} + \mathbf{E}_\psi^{++} \vec{\mathbf{S}}^{ext,+} \quad (68)$$

$$\psi_R^- = \mathbf{T}_\psi^{--} \vec{\mathbf{j}}^{-R} + \mathbf{R}_\psi^{-+} \vec{\mathbf{j}}^{+C} + \mathbf{E}_\psi^{--} \vec{\mathbf{S}}^{ext,-} + \mathbf{E}_\psi^{-+} \vec{\mathbf{S}}^{ext,+} \quad (69)$$

$$\psi_R^+ = \mathbf{R}_\psi^{+-} \vec{\mathbf{j}}^{-R} + \mathbf{T}_\psi^{++} \vec{\mathbf{j}}^{+C} + \mathbf{E}_\psi^{+-} \vec{\mathbf{S}}^{ext,-} + \mathbf{E}_\psi^{++} \vec{\mathbf{S}}^{ext,+} \quad (70)$$

The flux that will be created by merging the cells will be the average flux across the new cell  $(L + R)/2$ . To begin the process I add (47) to (49) and (48) to (50) which gives the following:

$$\begin{aligned} \psi_L^- + \psi_R^- = & \mathbf{T}_\psi^{--} \vec{\mathbf{j}}^{-C} + \mathbf{R}_\psi^{-+} \vec{\mathbf{j}}^{+L} + \mathbf{E}_\psi^{--} \vec{\mathbf{S}}^{ext,-} + \mathbf{E}_\psi^{-+} \vec{\mathbf{S}}^{ext,+} + \\ & \mathbf{T}_\psi^{--} \vec{\mathbf{j}}^{-R} + \mathbf{R}_\psi^{-+} \vec{\mathbf{j}}^{+C} + \mathbf{E}_\psi^{--} \vec{\mathbf{S}}^{ext,-} + \mathbf{E}_\psi^{-+} \vec{\mathbf{S}}^{ext,+} \end{aligned} \quad (71)$$

and:

$$\begin{aligned} \psi_L^+ + \psi_R^+ = & \mathbf{R}_\psi^{+-} \vec{\mathbf{j}}^{-C} + \mathbf{T}_\psi^{++} \vec{\mathbf{j}}^{+L} + \mathbf{E}_\psi^{+-} \vec{\mathbf{S}}^{ext,-} + \mathbf{E}_\psi^{++} \vec{\mathbf{S}}^{ext,+} + \\ & \mathbf{R}_\psi^{+-} \vec{\mathbf{j}}^{-R} + \mathbf{T}_\psi^{++} \vec{\mathbf{j}}^{+C} + \mathbf{E}_\psi^{+-} \vec{\mathbf{S}}^{ext,-} + \mathbf{E}_\psi^{++} \vec{\mathbf{S}}^{ext,+} \end{aligned} \quad (72)$$

Substituting (35) and (37) into both of these equations in order to eliminate the currents at the center boundary gives the following:

$$\begin{aligned}
\psi_L^- + \psi_R^- = & \mathbf{T}_{\psi}^{--} ((\mathbf{I} - \mathbf{R}_j^{-+} \mathbf{R}_j^{+-})^{-1} (\mathbf{T}_j^{--} \bar{\mathbf{j}}^{-R} + \mathbf{R}_j^{-+} \mathbf{T}_j^{++} \bar{\mathbf{j}}^{+L} \\
& + \mathbf{R}_j^{-+} \mathbf{E}_j^{+-} \bar{\mathbf{S}}^{ext,-} + \mathbf{R}_j^{-+} \mathbf{E}_j^{++} \bar{\mathbf{S}}^{ext,+} + \\
& \mathbf{E}_j^{--} \bar{\mathbf{S}}^{ext,-} + \mathbf{E}_j^{-+} \bar{\mathbf{S}}^{ext,+})) + \mathbf{E}_{\psi}^{-+} \bar{\mathbf{j}}^{+L} + \mathbf{E}_{\psi}^{--} \bar{\mathbf{S}}^{ext,-} + \mathbf{E}_{\psi}^{-+} \bar{\mathbf{S}}^{ext,+} + \\
& \mathbf{E}_{\psi}^{--} \bar{\mathbf{j}}^{-R} + \mathbf{E}_{\psi}^{-+} ((\mathbf{I} - \mathbf{R}_j^{+-} \mathbf{R}_j^{-+})^{-1} (\mathbf{R}_j^{+-} \mathbf{T}_j^{--} \bar{\mathbf{j}}^{-R} + \\
& \mathbf{R}_j^{+-} \mathbf{E}_j^{--} \bar{\mathbf{S}}^{ext,-} + \mathbf{R}_j^{+-} \mathbf{E}_j^{-+} \bar{\mathbf{S}}^{ext,+} \\
& + \mathbf{T}_j^{++} \bar{\mathbf{j}}^{+L} + \mathbf{E}_j^{+-} \bar{\mathbf{S}}^{ext,-} + \mathbf{E}_j^{++} \bar{\mathbf{S}}^{ext,+})) + \mathbf{E}_{\psi}^{--} \bar{\mathbf{S}}^{ext,-} + \mathbf{E}_{\psi}^{-+} \bar{\mathbf{S}}^{ext,+}
\end{aligned} \tag{73}$$

and:

$$\begin{aligned}
\psi_L^+ + \psi_R^+ = & \mathbf{R}_{\psi}^{+-} ((\mathbf{I} - \mathbf{R}_j^{-+} \mathbf{R}_j^{+-})^{-1} (\mathbf{T}_j^{--} \bar{\mathbf{j}}^{-R} + \mathbf{R}_j^{-+} \mathbf{T}_j^{++} \bar{\mathbf{j}}^{+L} + \\
& \mathbf{R}_j^{-+} \mathbf{E}_j^{+-} \bar{\mathbf{S}}^{ext,-} + \mathbf{R}_j^{-+} \mathbf{E}_j^{++} \bar{\mathbf{S}}^{ext,+} + \\
& \mathbf{E}_j^{--} \bar{\mathbf{S}}^{ext,-} + \mathbf{E}_j^{-+} \bar{\mathbf{S}}^{ext,+})) + \mathbf{T}_{\psi}^{++} \bar{\mathbf{j}}^{+L} + \mathbf{E}_{\psi}^{+-} \bar{\mathbf{S}}^{ext,-} + \mathbf{E}_{\psi}^{++} \bar{\mathbf{S}}^{ext,+} + \\
& \mathbf{R}_{\psi}^{+-} \bar{\mathbf{j}}^{-R} + \mathbf{T}_{\psi}^{++} ((\mathbf{I} - \mathbf{R}_j^{+-} \mathbf{R}_j^{-+})^{-1} (\mathbf{R}_j^{+-} \mathbf{T}_j^{--} \bar{\mathbf{j}}^{-R} + \\
& \mathbf{R}_j^{+-} \mathbf{E}_j^{--} \bar{\mathbf{S}}^{ext,-} + \mathbf{R}_j^{+-} \mathbf{E}_j^{-+} \bar{\mathbf{S}}^{ext,+} \\
& + \mathbf{T}_j^{++} \bar{\mathbf{j}}^{+L} + \mathbf{E}_j^{+-} \bar{\mathbf{S}}^{ext,-} + \mathbf{E}_j^{++} \bar{\mathbf{S}}^{ext,+})) + \mathbf{E}_{\psi}^{+-} \bar{\mathbf{S}}^{ext,-} + \mathbf{E}_{\psi}^{++} \bar{\mathbf{S}}^{ext,+}
\end{aligned} \tag{74}$$

I repeat the procedure outlined in Section II.C.1 for the current equations, collect the terms that act on the current coming in both sides of the cell, as well as the flux and rearrange to get new m matrices. For the  $\mathbf{m}^{\psi, in}$  matrix that acts on the current I get:

$$\begin{aligned}
\mathbf{T}_{\psi(i-1)}^{--} = & \mathbf{T}_{\psi(i)}^{--} (\mathbf{I} - \mathbf{R}_{j(i)}^{-+} \mathbf{R}_{j(i)}^{+-})^{-1} \mathbf{T}_{j(i)}^{--} \\
& \mathbf{T}_{\psi(i)}^{--} \bar{\mathbf{j}}^{-R} + \mathbf{R}_{\psi(i)}^{-+} (\mathbf{I} - \mathbf{R}_{j(i)}^{+-} \mathbf{R}_{j(i)}^{-+})^{-1} \mathbf{R}_{j(i)}^{+-} \mathbf{T}_{j(i)}^{--}
\end{aligned} \tag{75}$$

$$\begin{aligned}
\mathbf{R}_{\psi(i-1)}^{-+} = & \mathbf{T}_{\psi(i)}^{--} (\mathbf{I} - \mathbf{R}_{j(i)}^{-+} \mathbf{R}_{j(i)}^{+-})^{-1} \mathbf{R}_{j(i)}^{-+} \mathbf{T}_{j(i)}^{++} + \\
& \mathbf{R}_{\psi(i)}^{-+} + \mathbf{R}_{\psi(i)}^{-+} (\mathbf{I} - \mathbf{R}_{j(i)}^{+-} \mathbf{R}_{j(i)}^{-+})^{-1} \mathbf{T}_{j(i)}^{++}
\end{aligned} \tag{76}$$

$$\begin{aligned}
\mathbf{R}_{\psi(i-1)}^{+-} = & \mathbf{R}_{\psi(i)}^{+-} (\mathbf{I} - \mathbf{R}_{j(i)}^{-+} \mathbf{R}_{j(i)}^{+-})^{-1} \mathbf{T}_{j(i)}^{--} + \\
& \mathbf{R}_{\psi(i)}^{+-} + \mathbf{T}_{\psi(i)}^{++} (\mathbf{I} - \mathbf{R}_{j(i)}^{+-} \mathbf{R}_{j(i)}^{-+})^{-1} \mathbf{R}_{j(i)}^{+-} \mathbf{T}_{j(i)}^{--}
\end{aligned} \tag{77}$$

$$\begin{aligned}
\mathbf{T}_{\psi(i-1)}^{++} = & \mathbf{R}_{\psi(i)}^{+-} (\mathbf{I} - \mathbf{R}_{j(i)}^{-+} \mathbf{R}_{j(i)}^{+-})^{-1} \mathbf{R}_{j(i)}^{-+} \mathbf{T}_{j(i)}^{++} + \\
& \mathbf{T}_{\psi(i)}^{++} + \mathbf{T}_{\psi(i)}^{++} (\mathbf{I} - \mathbf{R}_{j(i)}^{+-} \mathbf{R}_{j(i)}^{-+})^{-1} \mathbf{T}_{j(i)}^{++}
\end{aligned} \tag{78}$$

Now the new  $\mathbf{m}^{\psi, in}$  matrix is:

$$\mathbf{m}^{\psi, in} = \begin{pmatrix} \mathbf{T}_{\psi(0)}^{--} & \mathbf{R}_{\psi(0)}^{-+} \\ \mathbf{R}_{\psi(0)}^{+-} & \mathbf{T}_{\psi(0)}^{++} \end{pmatrix} \quad (79)$$

Doing the same for the external emission source terms yields:

$$\begin{aligned} \mathbf{E}_{\psi(i-1)}^{--} &= \mathbf{T}_{\psi(i)}^{--} (\mathbf{I} - \mathbf{R}_{j(i)}^{-+} \mathbf{R}_{j(i)}^{+-})^{-1} \mathbf{R}_{j(i)}^{-+} \mathbf{E}_{j(i)}^{+-} + \\ &\quad \mathbf{E}_{j(i)}^{--} (\mathbf{I} - \mathbf{R}_{j(i)}^{-+} \mathbf{R}_{j(i)}^{+-})^{-1} \mathbf{E}_{\psi(i)}^{--} + \\ &\quad \mathbf{R}_{\psi(i)}^{-+} (\mathbf{I} - \mathbf{R}_{j(i)}^{+-} \mathbf{R}_{j(i)}^{-+})^{-1} \mathbf{R}_{j(i)}^{+-} \mathbf{E}_{j(i)}^{--} + \\ &\quad \mathbf{R}_{\psi(i)}^{-+} (\mathbf{I} - \mathbf{R}_{j(i)}^{+-} \mathbf{R}_{j(i)}^{-+})^{-1} \mathbf{E}_{j(i)}^{+-} + 2\mathbf{E}_{\psi(i)}^{--} \end{aligned} \quad (80)$$

$$\begin{aligned} \mathbf{E}_{\psi(i-1)}^{-+} &= \mathbf{T}_{\psi(i)}^{--} (\mathbf{I} - \mathbf{R}_{j(i)}^{-+} \mathbf{R}_{j(i)}^{+-})^{-1} \mathbf{R}_{j(i)}^{-+} \mathbf{E}_{j(i)}^{++} + \\ &\quad \mathbf{T}_{\psi(i)}^{--} (\mathbf{I} - \mathbf{R}_{j(i)}^{-+} \mathbf{R}_{j(i)}^{+-})^{-1} \mathbf{E}_{\psi(i)}^{-+} + \\ &\quad \mathbf{R}_{\psi(i)}^{-+} (\mathbf{I} - \mathbf{R}_{j(i)}^{+-} \mathbf{R}_{j(i)}^{-+})^{-1} \mathbf{R}_{j(i)}^{+-} \mathbf{E}_{j(i)}^{-+} + \\ &\quad \mathbf{R}_{\psi(i)}^{-+} (\mathbf{I} - \mathbf{R}_{j(i)}^{+-} \mathbf{R}_{j(i)}^{-+})^{-1} \mathbf{E}_{j(i)}^{++} + 2\mathbf{E}_{\psi(i)}^{-+} \end{aligned} \quad (81)$$

$$\begin{aligned} \mathbf{E}_{\psi(i-1)}^{+-} &= \mathbf{R}_{\psi(i)}^{+-} (\mathbf{I} - \mathbf{R}_{j(i)}^{-+} \mathbf{R}_{j(i)}^{+-})^{-1} \mathbf{R}_{j(i)}^{-+} \mathbf{E}_{\psi(i)}^{+-} + \\ &\quad \mathbf{R}_{\psi(i)}^{+-} (\mathbf{I} - \mathbf{R}_{j(i)}^{-+} \mathbf{R}_{j(i)}^{+-})^{-1} \mathbf{E}_{j(i)}^{--} + \\ &\quad \mathbf{T}_{\psi(i)}^{++} (\mathbf{I} - \mathbf{R}_{j(i)}^{+-} \mathbf{R}_{j(i)}^{-+})^{-1} \mathbf{R}_{j(i)}^{+-} \mathbf{E}_{j(i)}^{--} + \\ &\quad \mathbf{T}_{\psi(i)}^{++} (\mathbf{I} - \mathbf{R}_{j(i)}^{+-} \mathbf{R}_{j(i)}^{-+})^{-1} \mathbf{E}_{j(i)}^{+-} + 2\mathbf{E}_{\psi(i)}^{+-} \end{aligned} \quad (82)$$

$$\begin{aligned} \mathbf{E}_{\psi(i-1)}^{++} &= \mathbf{R}_{\psi(i)}^{+-} (\mathbf{I} - \mathbf{R}_{j(i)}^{-+} \mathbf{R}_{j(i)}^{+-})^{-1} \mathbf{R}_{j(i)}^{-+} \mathbf{E}_{j(i)}^{++} + \\ &\quad \mathbf{R}_{\psi(i)}^{+-} (\mathbf{I} - \mathbf{R}_{j(i)}^{-+} \mathbf{R}_{j(i)}^{+-})^{-1} \mathbf{E}_{j(i)}^{-+} + \\ &\quad \mathbf{T}_{\psi(i)}^{++} (\mathbf{I} - \mathbf{R}_{j(i)}^{+-} \mathbf{R}_{j(i)}^{-+})^{-1} \mathbf{R}_{j(i)}^{+-} \mathbf{E}_{j(i)}^{-+} + \\ &\quad \mathbf{T}_{\psi(i)}^{++} (\mathbf{I} - \mathbf{R}_{j(i)}^{+-} \mathbf{R}_{j(i)}^{-+})^{-1} \mathbf{E}_{j(i)}^{++} + 2\mathbf{E}_{\psi(i)}^{++} \end{aligned} \quad (83)$$

Now the new merged-cell m matrix for flux due to external emission source is:

$$\mathbf{m}^{\psi, ext} = \begin{pmatrix} \mathbf{E}_{\psi(0)}^{--} & \mathbf{E}_{\psi(0)}^{-+} \\ \mathbf{E}_{\psi(0)}^{+-} & \mathbf{E}_{\psi(0)}^{++} \end{pmatrix} \quad (84)$$

## REFERENCES

1. Carlson, B. G., *Solution of the Transport Equation by  $S_n$  Approximations*, Technical Report LA-1599, Los Alamos, NM: Los Alamos Scientific Laboratory, 1953
2. Carlson, B. G., “*Numerical Solution of Neutron Transport Problems*,” Proceeding of the American Mathematical Society, Vol. XI, 1961.
3. Carlson, B. G., Lathrop, K. D., “*Properties of New Numerical Approximations to the Transport Equation*”, Journal of Quantum Spectroscopic Radiation Transfer, 11:921-948, 1971
4. Davison, B, *Neutron Transport Theory*, Clarendon Press, Oxford, 1957
5. Dishaw, J, *Time Dependant Discrete Ordinates Neutron Transport Using Distribution Iteration in XYZ Geometry*, PhD dissertation, Air Force Institute of Technology, Wright-Patterson AFB, OH, September 2007.
6. Larsen, E. W., Alcouffe, R. E., “*The Linear Characteristic Method for Spatially Discretizing the Discrete Ordinates Equations in (X,Y)-Geometry*,” Proc. Int. Topl. Mtg. Advances Mathematical Methods for the Solution of Engineering Problems, Munich, Germany, April 27-29, 1981, Vol I, p. 99, American Nuclear Society (1981)
7. Lathrop, K. D, “*Ray Effects in Discrete Ordinates Equations*,” Nuclear Science and Engineering, 32:357-369, 1968
8. Lathrop, K. D., “Spatial Differencing of the Transport Equation: Positivity vs. Accuracy,” Journal of Computational Physics, 4:475–498 1969.
9. Lathrop, K. D., “*Remedies for Ray Effects*”, Nuclear Science and Engineering, 45:255-268 1971
10. Lewis, E.E and Miller, W.F, *Computational Methods of Neutron Transport*, American Nuclear Society, Inc., La Grange Park, Il, 1993.
11. Mathews, K. A., Professor of Nuclear Engineering, Air Force Institute of Technology, Wright-Patterson Air Force Base, OH, Personal Correspondence with J. Dishaw, 2008

12. Mathews, K. A., Professor of Nuclear Engineering, Air Force Institute of Technology, Wright-Patterson Air Force Base, OH, Personal Interview
13. Mathews, K. A., “*On the Propagation of Rays*”, Nuclear Science and Engineering, 132:155-180, 1999
14. Mathews, K., Dishaw, J., Wager, N., Prins, N., “*Adaptive Partial-Current Discrete Ordinates Radiation Transport with Distribution Iteration: An Alternative to Source Iteration*”, Nuclear Science and Engineering, 163:191-214, 2009
15. Mathews, K., Sjoden, G., and Minor, B., *Exponential Characteristic Spatial Quadrature for Discrete Ordinates Neutral Particle Transport in Slab Geometry*, Master’s Thesis, Air Force Institute of Technology, Wright-Patterson AFB, OH, March 1992.
16. Pang, Tao, *An Introduction to Computational Physics*, Cambridge University Press, New York, September 1997
17. Prins, N.J., *Distribution Iteration: A Robust Alternative to Source Iteration for Solving the Discrete Ordinates Radiation Transport Equations in Slab and XY-Geometries*. PhD dissertation, Air Force Institute of Technology, Wright-Patterson AFB, OH, March 2008
18. *Slab Geometry Discrete Ordinates Code*, Version 0.8, Computer Software, K.A. Mathews, Air Force Institute of Technology, Wright-Patterson Air Force Base, OH, 2010
19. Wager, N.J., *A Rapidly-Converging Alternative to Source Iteration for Solving the Discrete Ordinates Transport Equations in Slab Geometry*. PhD dissertation, Air Force Institute of Technology, Wright-Patterson AFB, OH, March 2004.



<b>REPORT DOCUMENTATION PAGE</b>				Form Approved OMB No. 074-0188	
<p>The public reporting burden for this collection of information is estimated to average 1 hour per response, including the time for reviewing instructions, searching existing data sources, gathering and maintaining the data needed, and completing and reviewing the collection of information. Send comments regarding this burden estimate or any other aspect of the collection of information, including suggestions for reducing this burden to Department of Defense, Washington Headquarters Services, Directorate for Information Operations and Reports (0704-0188), 1215 Jefferson Davis Highway, Suite 1204, Arlington, VA 22202-4302. Respondents should be aware that notwithstanding any other provision of law, no person shall be subject to a penalty for failing to comply with a collection of information if it does not display a currently valid OMB control number.</p> <p><b>PLEASE DO NOT RETURN YOUR FORM TO THE ABOVE ADDRESS.</b></p>					
<b>1. REPORT DATE (DD-MM-YYYY)</b> 25-03-2010		<b>2. REPORT TYPE</b> Master's Thesis		<b>3. DATES COVERED (From – To)</b> Aug 2008 – Mar 2010	
<b>4. TITLE AND SUBTITLE</b>  Improving Low Order, Linear, Positive Spatial Quadratures for the Partial Current Neutron Transport Method				<b>5a. CONTRACT NUMBER</b>	
				<b>5b. GRANT NUMBER</b>	
				<b>5c. PROGRAM ELEMENT NUMBER</b>	
<b>6. AUTHOR(S)</b>  Snyder, John M., MAJ, USA				<b>5d. PROJECT NUMBER</b> ENP10M-08	
				<b>5e. TASK NUMBER</b>	
				<b>5f. WORK UNIT NUMBER</b>	
<b>7. PERFORMING ORGANIZATION NAMES(S) AND ADDRESS(S)</b> Air Force Institute of Technology Graduate School of Engineering and Management (AFIT/EN) 2950 Hobson Way WPAFB OH 45433-7765				<b>8. PERFORMING ORGANIZATION REPORT NUMBER</b>  AFIT/GNE/ENP/10M-08	
<b>9. SPONSORING/MONITORING AGENCY NAME(S) AND ADDRESS(ES)</b> Intentionally Left Blank				<b>10. SPONSOR/MONITOR'S ACRONYM(S)</b>	
				<b>11. SPONSOR/MONITOR'S REPORT NUMBER(S)</b>	
<b>12. DISTRIBUTION/AVAILABILITY STATEMENT</b> APPROVED FOR PUBLIC RELEASE; DISTRIBUTION UNLIMITED.					
<b>13. SUPPLEMENTARY NOTES</b> This material is declared a work of the U.S. Government and is not subject to copyright protection in the United States.					
<b>14. ABSTRACT</b> AFIT researchers have developed a new approach to solving Discrete Ordinates equations, which approximate the linear Boltzmann Transport Equation (BTE). The usual approach is von Neumann iteration on the scattering source, which requires repeated sweeps through the spatial-angular grid. Acceptable convergence requires complicated and expensive acceleration schemes. The new approach, Partial-Current Transport (PCT) with Adaptive Distribution Iteration, eliminates scattering source iteration through matrix inversions and a reduced-size global linear algebra problem. It creates the needed matrices directly from the standard spatial quadratures used in the sweeping. Positivity, linearity, and (higher-than-first-order) accuracy are the key desirable qualities with all Discrete Ordinates methods, but all three, according to Lathrop [8], cannot be achieved simultaneously. If a high order accurate, linear method is used, it can produce negative fluxes. Non-linear methods have been developed that are high-order accurate and positive, but these methods are not widely accepted because the BTE is itself a linear equation. Positive, linear methods are available, but are only first-order accurate. The latter can achieve needed accuracy by using optically-thin cells, but with Source Iteration (SI), this requires a fine grid of many cells, hence large computational expense. My new approach is to partition an optically thick cell into 2N identical sub-cells. Each sub-cell is optically thin enough that first-order accurate spatial quadrature methods are sufficiently accurate as well as being linear and positive. The needed matrices are computed as before for a (thinnest) sub-cell. My algorithm combines the matrices for a pair of sub-cells to get the matrices for a single (merged) sub-cell twice as thick. Merging N times yields the matrices for the original cell. This allows PCT to solve the discrete ordinates equations with linearity, positivity, and sufficient accuracy without the high computational cost of increasing the number of cells by a factor of 2N.					
<b>15. SUBJECT TERMS</b> Discrete Event Simulation, Dependency Injection, Hot Swapping, Unit Testing					
<b>16. SECURITY CLASSIFICATION OF:</b>			<b>17. LIMITATION OF ABSTRACT</b>  UU	<b>18. NUMBER OF PAGES</b>  65	<b>19a. NAME OF RESPONSIBLE PERSON</b> Mathews, Kirk A., Professor of Nuclear Engineering
<b>REPORT</b> U	<b>ABSTRACT</b> U	<b>c. THIS PAGE</b> U			<b>19b. TELEPHONE NUMBER (Include area code)</b> (937) 255-3636, x4508